Desalination 583 (2024) 117695

Contents lists available at ScienceDirect

Desalination

journal homepage: www.elsevier.com/locate/desal

Advances in capacitive deionization (CDI) systems for nutrient recovery from wastewater: Paving the path towards a circular economy

Mohsen Askari [a,b], Saeid Rajabzadeh [a], Leonard Tijing [a,b], Ho Kyong Shon [a,b,*]

[a] Centre for Technology in Water and Wastewater, School of Civil and Environmental Engineering, University of Technology Sydney, P.O. Box 123, 15 Broadway, NSW 2007, Australia
[b] ARC Research Hub for Nutrients in a Circular Economy, University of Technology Sydney, PO Box 123, 15 Broadway, Ultimo, New South Wales 2007, Australia

HIGHLIGHTS

- Faradic materials boost CDI for nutrient recovery.
- Optimizing parameters crucial for high-efficiency nutrient recovery in CDI
- CDI opens a highly efficient path for circular economy development.
- CDI exhibits high ammonia recovery potential.
- Combined N and P recovery shows cost-effective potential.

GRAPHICAL ABSTRACT

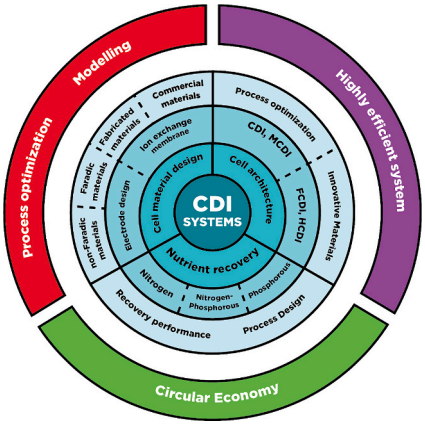

ARTICLE INFO

Keywords:
Capacitive deionization
Nutrient recovery
Nitrogen
Phosphorus
Wastewater

ABSTRACT

The escalating global population growth, the aspiration for improved living standards, environmental concerns, and the rising focus on circular economy frameworks have collectively emphasized the imperative to recover resources such as nutrients, water, and energy. Despite the notable advantages and technological capabilities of capacitive deionization (CDI) systems, their potential remains largely untapped. This comprehensive review aims to synthesize and analyze the progress made in CDI systems for nutrient recovery. It concentrates on two vital wastewater nutrients: nitrogen (N) and phosphorus (P). The study explores both conventional and advanced CDI systems, including CDI, membrane capacitive deionization (MCDI), flow electrode capacitive deionization (FCDI), and hybrid capacitive deionization (HCDI). In three key areas, a detailed framework for recovering nitrogen, phosphorus, and both is provided: (1) process optimization, (2) innovative cell design, and (3) process development for effectively integrating CDI with complementary techniques, enabling simultaneous ion recovery and the production of value-added products. Additionally, future perspectives on CDI development and

* Corresponding author at: Centre for Technology in Water and Wastewater, School of Civil and Environmental Engineering, University of Technology Sydney, P.O. Box 123, 15 Broadway, NSW 2007, Australia.

https://doi.org/10.1016/j.desal.2024.117695
Received 25 December 2023; Received in revised form 19 April 2024; Accepted 25 April 2024
Available online 27 April 2024

expansion for nutrient recovery are discussed in this review with an emphasis on aligning these efforts with circular economy goals.

1. Introduction

The global population will grow by over 20 % by 2050, and food demand will increase by 60 % compared to 2005. As a result of a disparity between dietary nutrient requirements and supply, there is still a nutrient deficit at the country level. This is despite an even distribution among countries [1–3]. For human security, nitrogen (N) and phosphorus (P) are essential nutrients for food production. These nutrients are unevenly used across the world, with 80 % of African countries experiencing nitrogen scarcity. In addition 65 % of world phosphorus deficits are concentrated on just 10 % of cropland [4]. On the other hand, it is estimated that N pollution costs the global economy 200–2000 USD billion annually, equivalent to 0.2 %–2 % of global GDP [2]. As a result, environmental pollution, biodiversity loss, climate change, and stratospheric ozone depletion have increased locally, regionally, and globally [2,5,6]. In light of the limited natural availability of phosphorus as a non-renewable resource, recovering it is of paramount importance [7]. Moreover, the current fertilizer price crisis serves as a poignant reminder for the worldwide community that phosphorus needs to be addressed proactively [8].

Wastewater nutrient recovery technologies, such as separating residues into liquid and solid phases, offer a novel way to approach this problem [4,9]. Aside from supporting fertilizer production, it also ensures a stable supply of food, prevents environmental damage caused by the release of these ions into the environment (see Fig. 1) [7,10], and provides a practical and cost-effective solution. However, wastewater technologies encounter significant challenges and are not well-suited for nutrient recovery from waste streams. Some of the challenges include high energy consumption in membrane-based solutions, selectivity issues with ion exchange membranes, slow adsorption kinetics and sludge production in physical adsorption methods, high operational costs of stripping towers and membrane contractors due to the large quantities of chemicals needed to raise pH, low current densities produced by bacteria, and a lack of selectivity in bio-electrochemical system [11–14]. In recent years, electrochemical advances [12] have made capacitive deionization (CDI) an attractive electrosorption desalination technology, offering eco-friendliness, significantly reduced energy consumption [15], and energy recovery [16]. CDI technology is an electrically driven desalination method with low voltage that provides enhanced energy efficiency [17]. In addition to achieving high overall energy efficiency, CDI also offers facile electrode regeneration, no secondary pollution, and partial energy recovery, in addition to enhancing electrode regeneration. This makes it economically feasible and energy-effective [18].

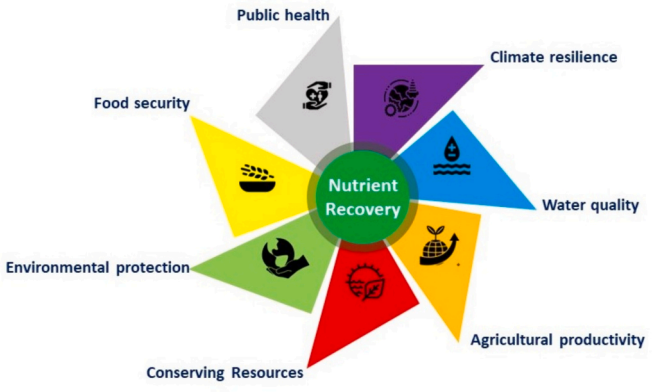

Fig. 1. Illustration of the significance of nutrient recovery.

Fig. 2(a) illustrates the upward trend in CDI system developments over the past 15 years (2009–2023). Although CDI is widely recognized as an effective electrical desalination technology, its performance is limited due to scale-up issues [17,19]. In addition, CDI is limited in its ability to eliminate neutral organic substances, requiring its use in combination with complementary methods [20,21].

The literature extensively discusses CDI systems for desalinating seawater or brackish water, but these systems are not cost-effective. Various applications of CDI-based systems have been explored in recent years across a wide range of fields. These systems, especially in the realm of selective ion removal, have demonstrated significant advancements [12,22,23]. Research in CDI has been extended to encompass applications in water softening, removal of organic contaminants, extraction of heavy metals, CO_2 capture, and recovery of resources, including nutrients such as nitrogen and phosphorus [12,18,20,24–26]. Given its potential for nutrient treatment, CDI emerges as a focal point for innovative research. Although the importance of selective nutrient recovery [16,17], efficient ion removal [21,27], capturing soluble gases like CO_2 [28], and integrating with other systems [20] is emphasized, it is worth noting that nutrient recovery through CDI is still in its early stages. As Fig. 2(b) shows, the literature on CDIs for nutrient recovery focuses on nitrate removal. However, in recent years, increasing attention has been given to phosphorus removal and the simultaneous removal of both ions.

Herein, a thorough examination of CDI components and systems is undertaken in Section 2 to elucidate the historical progress of these systems. Section 3 summarizes the advancements made in leveraging CDI systems for the removal of nitrogen and phosphorus from wastewater, along with the simultaneous recovery of these elements. Various system configurations and performance metrics are explored. Additionally, both the potential and opportunities of CDI systems in the context of nutrient recovery processes are thoroughly discussed. The primary objective is to demonstrate how these technologies facilitate circular waste resource utilization by creating value-added products. To conclude, recommendations for future research and perspectives on further advancements in this field are provided in this review. The most notable advancements within their respective domains are also highlighted, and our view on those that offer the most potential for future research is presented.

2. Advancements in capacitive deionization systems

There is a wealth of literature available regarding electrode materials, ion exchange membranes, cell designs, operational modes, and theoretical models of different CDI architectures [29–35]. As an initial step in addressing the question of how CDI systems can efficiently facilitate nutrient recovery, we highlight the most notable advances in their respective fields. Perspectives that could contribute to innovative pathways and the future of nutrient recovery systems will be presented.

Electrochemistry captures anions and cations on positive and negative electrodes, respectively. It releases them back into the electrolyte to regenerate the electrodes. Consequently, the effluent produced can be separated into deionized and concentrated streams [12]. In a CDI system (Fig. 3(a)), the applied electrical potential between porous electrodes drives charged particles to accumulate in the Electrical Double Layer (EDL) [36]. This leads to changes in the electrode surface charge, causing polarization and ion adsorption [12]. Conventional CDI operates without electron transfer through redox pairs, relying on EDL-mediated ion adsorption and desorption [12]. The physicochemical attributes of electrodes significantly influence adsorptive performance, as affirmed by the Gouy-Chapman-Stern (GCS) model and the Modified

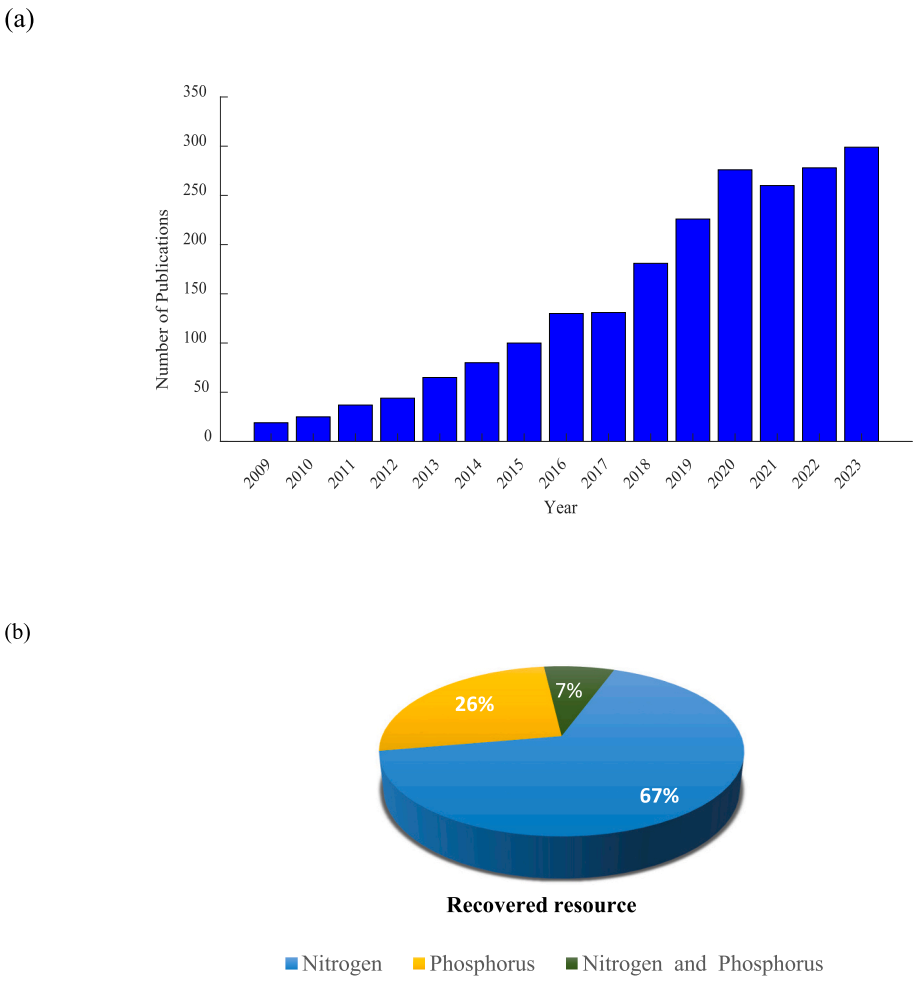

Fig. 2. (a) Number of peer-reviewed papers in the "CDI "field per year (2009–2023) based on the Web of Science database (keywords: capacitive deionization, CDI, MCDI, FCDI, HCDI), (b) percentage of publications with nutrient recovery perspective.

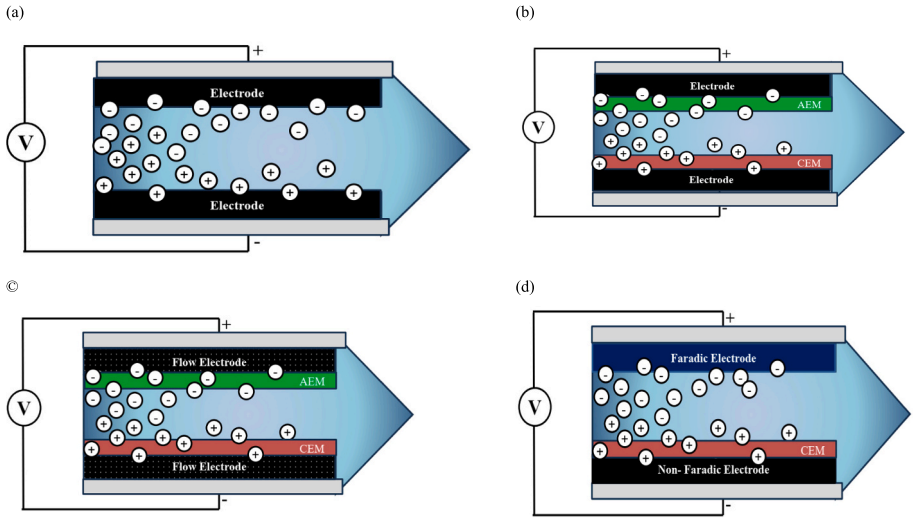

Fig. 3. Representative schematic diagram of (a) classic capacitive deionization (CDI); and (b) membrane capacitive deionization (MCDI). (c) Flow electrode capacitive deionization (FCDI); (d) hybrid capacitive deionization (HCDI).
(Adapted from [20]).

Donnan model, with these models instrumental in comprehending ion behaviour and charge distribution at the electrode-electrolyte interface. These models play a vital role in the design and optimization of CDI systems, contributing to advancements in their efficiency and performance [37,38].

Introducing ion-exchange membranes (IEMs) into capacitive

membrane deionization systems (CDI) (Fig. 3(b)) has been proposed as an approach to improve CDI efficiency while addressing challenges such as co-ion expulsion, electrode lifespan, and energy efficiency [36,39]. The MCDI process uses cation and anion exchange membranes to enhance charge transfer efficiency by allowing only counterions to pass through the membranes and be adsorbable within the electrode pores. In MCDI, counterions are not transported to the opposite electrode during reverse voltage desorption. Further electrosorption occurs in macropores due to co-ions trapped in macropores between the ion-exchange membranes and the porous electrodes [12,26]. The performance of bare carbon electrodes in ion separation has been enhanced by incorporating various modifications such as ion-exchange resins or membranes, functional groups, solid particles, metal oxide particles, resins [12], and electrically regenerated ion exchangers (ERI) [40]. IEM applications have grown rapidly in recent years [41–43], although few review papers have been published on them [44]. According to McNair et al. [44], four primary methods are used to fabricate ion-exchange membranes for MCDI: (a) blending ion-exchange materials with carbon particles in the electrode slurries before electrode coating (pre-electrode fabrication), (b) direct coating of ion-exchange materials onto pre-prepared electrodes (post-electrode fabrication), (c) solution casting and phase inversion of polymeric ion-exchange films, and (d) pore filling by incorporating ion-exchange polymers into porous membranes to provide ion transport channels.

The use of IEMs, however, may result in membrane fouling in MCDI, as operating conditions and modes are more diverse [20] than traditional CDI [31]. Moreover, the static electrodes used in MCDI have limitations concerning ion adsorption and are best suited to brines with low to medium ion concentrations rather than brines with high ion concentrations [20]. Ideally, MCDI energy consumption should be below 1 kWh/m^3 of fresh water produced to be competitive with reverse osmosis [45]. To tackle the issue of frequent charging and discharge in CDI, Jeon et al. [31] introduced Flow Electrode Capacitive Deionization (FCDI) employing a slurry electrode [46] (Fig. 3 (c) [20]). In addition to continuous operation without repetitive charging and discharging cycles, FCDI technology also enables electrode regeneration, enhancing operational flexibility, providing long-term continuous operation, and allowing for unlimited adsorption capacity [18,20,22,46–48]. The activated carbon particles in slurry electrodes show higher electrosorption capacity in FCDI compared to MCDI electrodes [20]. FCDI is also capable of desalinating saline waters with a concentration of 35,000 mg/L, in addition to desalinating brines with high total dissolved solids (TDS) [49]. Lee et al. introduced a hybrid capacitive deionization (HCDI) system that combines the principles of CDI with an asymmetric capacitive system utilizing battery materials [48]. An electrochemical reaction captures sodium ions instead of EDL on one side of an HCDI electrode (Fig. 3(d)). On the other side, carbon-based materials are used to physically adsorb chloride ions [50,51]. This system offers several advantages over previous approaches. Compared to standard MCDI and FCDI configurations, HCDI offers increased salt removal capacity, improved energy efficiency, and enhanced scalability [52,53].

In recent years, significant progress has been made in advancing high-performance CDI systems. This progress is driven by the strategic integration of cutting-edge electrode materials, pioneering ion-exchange membranes (IEMs), and innovative cell designs. These dynamic advancements have significantly elevated system functionalities, particularly inefficient ion separation and enhanced energy efficiency.

Capacitive electrodes are employed in non-Faradaic ion separation, with CDI being a prominent technology in this category. Traditionally, carbon-based materials have been used for non-Faradaic systems. Non-Faradaic materials, which operate through capacitive mechanisms, are preferred due to their cost-effectiveness, ease of synthesis, and rapid ion transportation. Nevertheless, these materials exhibit restricted charge storage capacity (typically below 20 mg/g), suboptimal cycling stability (usually permitting only 10–20 cycles), and an inability to selectively remove ions [54–56].

In the past decade, significant advancements have been made in ion separation by developing various capacitive [57], batteries [58,59], or hybrid materials [20]. There has been extensive literature on the electrochemical properties of carbon-based materials and structures, which has been crucial to developing non-Faradaic electrodes [60]. Numerous carbon [59] materials including activated carbon (AC) [61,62], carbon aerogel [63,64], mesoporous carbon [65,66], pure carbon cloth [67] modified carbon cloth [68], carbon nanotubes (CNTs) [69,70], graphene [71–73], ion exchange coated carbon electrodes [74], composite of carbon nanofibers [75,76] and other carbon-based composites [77,78] and nanocomposites [79–81] have greatly improved the functional performance of these electrodes. Enhancing non-Faradaic capacitive ion storage typically requires electrodes with high surface area, well-distributed pores, good electrical conductivity, and chemical stability [31]. To address the inevitable side reactions associated with carbon electrodes, such as the oxidation of carbon anodes [31] and the co-ion expulsion effect [82], the adoption of Faradaic electrodes has been suggested [83]. Faradaic materials function through a pseudocapacitive or intercalation mechanism, offering substantial ion storage capacity and selective ion-capturing properties. This makes Faradaic ion separation advantageous, as it enables larger storage capacity and selective ion separation characteristics. Through intercalation between electrode layers, within the lattice, or redox reactions with ions, the Faradaic electrode captures ions. It reduces ion migration resistance and improves energy efficiency [12,84]. In the case of Faradaic electrodes, progress has been documented in the development of highly selective adsorption materials, enabling the targeted separation of specific ions from ionic mixtures. Common Faradaic electrodes have utilized two-dimensional MXenes [85,86], three-dimensional Prussian blue analogues (PBAs) [87,88], $NaTi_2(PO_4)_3$ [89,90], $NaMnO_2$ (NMO) [91,92], λ-MnO_2/AC [94], iron-based phosphate [95], ZrO_2 [96], RuO_2 [97], and hexacyanoferrate materials [98]. Diverse types of Faradaic reactions within CDI systems can result in reduced electrode performance, lowered energy efficiency, and shortened electrode lifespan. Conversely, certain reactions have shown the potential to improve desalination performance by leveraging pseudocapacitive/intercalation effects and generating charged species [31]. According to research conducted by Leong et al. [99], it was found that Faradic electrode materials exhibit significantly higher salt removal capacities (over 40 mg/g) compared to carbon materials, which typically demonstrate capacities around 15 mg/g.

Using Faradic reactions via redox intercalation or crystalline phase transformation, Pasta et al. [100] presented the concept of a battery deionization system (BDI), which is similar to lithium-ion batteries, for desalination. As opposed to CDI, the BDI system stores cations and anions within the cathode and anode, rather than in the EDL. In addition to its high ion removal capacity, DBI is highly efficient and requires minimal overall energy. To achieve this, a small voltage window during the desalination process is applied to avoid significant co-ion expulsion and parasitic reactions [100–102].

The literature also presents various fabrication-based strategies to enhance the electrochemical performance, and functionality of electrodes in CDI systems [12,103–105]. For instance, the utilization of polymer electrodes with superior electrochemical performance, such as conductive polymers with high capacitance storage capacity, has led to improved ion removal efficiency. Additionally, significant increases in CDI electrode capacitance have been achieved by incorporating polyaniline (PANI) [106] and polypyrrole (PPy) [107], surfactant-functionalized conductive PPy [108], and conductive composites [70,108–110]. Moreover, researchers have explored the introduction of redox-active molecules or exploited the properties of polymers to reversibly switch the interaction of neutral species with electrodes through an electric field [111]. There have also been reports of free-standing nanofibrous electrodes being able to enhance the efficiency of CDI as promising platforms for future CDI research [112–114]. The promising outcome for desalination has emerged from the blending of

Table 1
Challenge of current technologies for nitrate and ammonia removal.

Technology	Challenge	Ref
Biological	Significant retention times	[26]
	High sludge volume generation (secondary pollution)	[22,26]
	Requires large-scale installations	[117]
	Slow ion removal kinetics	[117]
	High sensitivity to pH and temperature	[117]
Physical-chemical	Expensive and limited recoverability of popular adsorbent.	[26]
	Inefficient removal of ions by membrane-based processes.	[118]
	High energy demand for membrane-based technologies	[117]
	High operational cost	[22]

Faradic materials with capacitive materials, exemplified by the combination of RuO_2 and activated carbon to create a composite electrode [97].

3. Application of CDIs in nutrient recovery

Although common biological and physical-chemical technologies can recover nitrogen and phosphorus from resources, they present significant challenges (as presented in Table 1), and many of them have not been commercialized [115]. Regarding the use of CDI, research results indicate its promise as a solution for recovering nitrogen and phosphorus from wastewater. Nevertheless, there is a need to investigate methods to enhance the selectivity and nutrient recovery capabilities of CDI, transitioning from a preliminary stage to a more detailed examination [116].

In the upcoming sections, the domain of CDI systems is delved into, with their capabilities and potential for nutrient recovery being examined. Accordingly, the literature on nutrient recovery applications for CDI, MCDI, FCDI, and HCDI was reviewed from three perspectives: (1) the effect of process parameters, covering all effective parameters on nutrient capture; (2) cell design, focusing on engineering the CDI cell and the effects of its components to advance CDI systems; and (3) process development, exploring the design of stages and integrated/hybrid systems to achieve high-performance removal and recovery of nutrient ions. Tables 2, 3, and 4 contain detailed information regarding CDI systems for the recovery of nitrogen, phosphorus, and nitrogen-phosphorous ions, including cell design, wastewater source, ion type recovered, operation voltage, energy consumption, and system performance.

3.1. Nitrogen recovery

3.1.1. CDI and MCDI

3.1.1.1. Effect of process parameters. The electrosorption capacity depends on various operational parameters, comprising cell voltage, solution flow rate, pH, feed temperature, electrode thickness, initial salt concentration, operational mode (batch/single pass), adsorption method (constant current/voltage), CDI unit geometry (e.g., flow by, flow through), and desorption method (zero/reverse voltage) [24,29,30]. Furthermore, specific capacitance, pore structure, electrical conductivity, and the concentration of binder in the ion exchange membrane can have a significant impact on the process. For optimizing selective removal efficiency in desalination, comprehensive conclusions regarding CDI process's operational parameters can be drawn. However, nutrient recovery requires more consideration to recognize the effectiveness of relevant parameters.

One study examined the influence of co-existing anions on the selective removal of nitrates and ammonium ions in CDI [119] and MCDI [120]. The investigations aimed to identify optimal parameters that can enhance the performance of nitrogen recovery from CDI systems [121,122]. AC electrodes are used in CDI for the removal and recovery of nitrate ions under conditions that mimic real municipal wastewater treatment. The findings demonstrated a 21 % recovery efficiency for nitrate ions from low-salinity water, coupled with a removal efficiency of 48 %. However, it is imperative to highlight that the existence of competitive ions in the solution resulted in a marginal decrease of approximately 10 % in the nitrate removal efficiency [123].

The capability of CDI and MCDI to preferentially select nitrate (NO_3^-) over chloride (Cl^-) was also examined [124]. In CDI factors like charging time, the initial concentration ratio of Cl^-, and applied voltage exert influence on selectivity. Longer charging times and higher NO_3^-/Cl^- ratios increased selectivity while increasing the applied voltage reduced it. In MCDI, the presence of an ion-exchange membrane reduced selectivity compared to CDI. The study also explored single-solute and binary-solute solutions, finding that NO_3^- preferentially adsorbed over Cl^- in CDI. The researchers identified a two-step competitive electrosorption process during charging. The findings provide insights into ion selectivity in electrosorption and highlight the trade-off between selectivity and ion removal capacity in CDI and MCDI. Considerable research has also been conducted to comprehensively explore the application of CDI to separate ions from an aqueous solution of ammonium perchlorate (NH_4ClO_4) [84]. The findings show that both NH_4^+ and ClO_4^- and ions can be effectively eliminated. The report indicates that approximately 95 % of the NH_4ClO_4 ions were successfully removed until the carbon aerogel electrodes reached their saturation point.

3.1.1.2. Cell design. To select nitrate ions from solutions containing different types of anions, ion exchange electrodes in the CDI system were compared to electrodes in MCDI systems. An anion exchange resin, BHP55, was used to coat a carbon electrode to create a composite carbon electrode. Compared to the MCDI system (constructed with ion exchange membranes and carbon electrodes), the coated electrode in the CDI system exhibited 2.3 times more nitrate ion adsorption [125]. The enhanced adsorption was attributed to the initial electrostatic attraction of ions, followed by ion exchange reactions between the resin powder and the mixed anions solution. Ion exchange-electrochemical cells were found to adsorb about twice as many nitrate ions as carbon electrodes without anion exchange polymer cells in desalination experiments with mixed chloride, nitrate, and sulphate ions [126]. In contrast, chloride and sulphate ions were adsorbable in both cells in the same amount. Chelating resin suggested as a possible means of effectively removing heavy metals [122] and as a critical factor influencing ion selectivity [125,126].

Kim et al. [127] conducted experiments to assess the effectiveness of the nitrate recovery and desalination process. Carbon electrodes coated with a polymer selective for anions, along with polystyrene macroporous A520E resin particles, were utilized in MCDI (A520E/IX layered electrode). The preferential electrosorption performance species followed the order of $NO_3^- > SO_4^{2-} > Cl^-$ for both the IX layered (control anode) and A520E/IX layered electrodes. The results revealed that the removal rate reached 81.5 %, indicating a superior selectivity for nitrate removal from actual municipal wastewater. The authors also evaluated polymer-coated carbon electrodes in MCDI systems for wastewater reuse [128]. The findings demonstrated notable improvements in sorption capacities and charge efficiencies, further highlighting the efficacy of these electrodes in enhancing the performance of wastewater treatment processes. The pilot-scale MCDI system demonstrated efficient removal of anions from municipal wastewater, with the highest removal efficiency observed for Cl^- followed by NO_3^- and then SO_4^{2-}. Additionally, the coated electrodes exhibited excellent regeneration capability during 15-day operation. The performance of the system was particularly notable in removing NO_3^-, achieving a removal rate of up to 91.08 %. These results confirmed the effectiveness of electrode modification in

Table 2
System design for CDI, MCDI, and i-CDI systems for selective recovery of nitrogen from wastewater.

Cell design	Source	Ion recovered	Operation voltage (V)	Energy consumption	System performance	Ref.
Two copper hexacyanoferrate (CuHCF) battery electrodes, commercial AEM	Synthetic wastewater, actual domestic wastewater	NH_4^+	0.1, 0.2	1.5 kWh/kg N	Selectivity (ratio of percent removed of $NH_4^+/Na^{+)} > 5$ for synthetic wastewater, selectivity >4 for actual domestic wastewater (85 % removal)	[11]
AC-based electrode	Prefiltered tap water	NO_3^-, NH_4^+	1.25 per stack	0.45–5.35 kWh/m^3	98 % NO_3^- removal, 71.9 %–88.1% N removal	[119]
AC-based electrode	Brackish groundwaters	NO_3^-	1.6	1.2308 kWh/m^3	Efficient removal of NO_3^- in the presence of relatively high concentrations of NaCl and co-existing anions	[141]
Carbon electrode coated by the anion exchange resin, BHP55 IEX resin	Mixing solution of NaCl and $NaNO_3$	NO_3^-	1.0	N/A	Adsorption capacity is 2.3 times greater than that of the MCDI system.	[120]
Carbon electrode coated by the anion exchange resin, BHP55 IEX resin	Mixing solution of NaCl, $NaNO_3$, and Na_2SO_4	NO_3^-	1.0	N/A	Two-fold higher adsorption of NO_3^- in MCDI compared to the CDI one, same adsorption of chloride and sulphate ions in both cells	[126]
AC-based electrode	Mixing solution of multi-ions	NO_3^-, NH_4^+	1.2	N/A	The highest efficiency and NH_4^+ in competition between monovalent anions (Cl^-, F^-, and Br^-) and cations (Na^+, K^+)	[122]
AC-based electrode, phenol formaldehyde IEX resin	A multi-ionic solution containing monovalent, divalent, and trivalent anions	NO_3^-	1.2	N/A	Normalized equivalent capacity order: trivalent anion > divalent anion > monovalent anion, Cl^- is preferably electrosorbed over NO_3^- at the beginning and end of the electrosorption process, some Cl^- ions are exchanged for NO_3^-	[121]
Carbon aerogel electrodes	An aqueous solution of ammonium perchlorate (NH_4ClO_4)	NH_4^+	1.2	4.5 J/mo1 at 0.6 V, and 9.0 J/mo1 at 1.2 V	Effective removal of NH_4^+ and ClO_4^- ions, and approximately 95 % removal of NH_4ClO_4 ions	[84]
Ultra microporous aerogel monolith (μHCAM)	Synthetic wastewater	NO_3^-	±0.6, ±0.8, ±1	N/A	NO_3^- prefers to electrosorption over sulfate and chloride due to tightly distributed micropores (predominantly <1 nm)	[134]
AC electrode	Synthetic wastewater	NO_3^-	1.2	N/A	21 % recovery from low-salinity water, 48 % removal efficiency, and 10 % decrease in removal efficiency due to co-existing ions	[123]
AC/PVDF/polyaniline/ZrO_2	Single salt ($NaNO_3$) Binary salt ($NaNO_3$/NaCl)	NO_3^-	2	N/A	Electrosorption capacity 6.01 mg/g, removal efficiency of 60.01 %, water recovery of 72.94 %	[135]
Two uncoated carbon fibre sheets, or a SiO_2-coated sheet as the working electrode and an γ-Al_2O_3-coated sheet as the counter electrode	Synthetic wastewater	NO_3^-	1.5	N/A	Coated electrodes likely enhance nitrate removal by promoting faster ion transport through reduced hydrophobicity and increased surface area.	[117]
AC-based electrodes, BHP55 IEX resin	Synthetic wastewater	NO_3^-	1–1.6	N/A	2.3 times higher adsorption of NO_3^- in nitrate-selective composite carbon electrodes greater than the adsorption in the MCDI	[136]
AC-based electrodes, modified AC with phosphoric acid (ACP)	Synthetic wastewater	NO_3^-	1.4	N/A	ACP electrodes exhibited a 22.26 % higher nitrate removal rate compared to AC electrodes	[129]
i-CDI, AC electrode, functionalized cathode with cationic surfactant cetrimonium bromide (CTAB)	Synthetic wastewater	NO_3^-	<4 V for reduction of NO_3^- to NO_2^-	N/A	Adsorption capacity of about 80 mg/g of activated carbon, access to approximately 40 % of the initial electrode capacity, following electrical regeneration	[131]
i-CDI, AC electrode, functionalized cathode with cetrimonium bromide (CTAB) and anode with dodecyl benzene sulphonate (SDBS)	Pure sodium nitrate	NO_3^-	0 for adsorption, 0.2–1.4 for regeneration step	0.07 kWh/m^3 at 1.4 V re-generation voltage with ~30 % salt removal	Maximum removal of 10 mg of sodium nitrate per gram of both electrodes.	[132]
i-CDI, AC electrode, functionalized cathode with cetrimonium bromide (CTAB) and anode with dodecyl benzene sulphonate (SDBS)	Synthetic wastewater	NO_3^-	1 V in regeneration and 0 V in adsorption steps	N/A	The inherent selectivity of CTA-AC for nitrate over chloride is approximately 7.7	[133]
AC-based electrodes, commercial CEM and AEM	Synthetic wastewater	NO_3^-	1.0 per stack	N/A	High selectivity of AMX membrane for nitrate ions with a selectivity coefficient (NO_3^-/Cl^- ratio) of 4.37	[120]
Graphene laminate (GL) electrodes	Synthetic wastewater	NH_4^+	2	N/A	Removal of 15.3 mg/g NH_4Cl, a faster rate of onions adsorption on an on GLs than Na^+ ions	[26]

(*continued on next page*)

Table 2 (*continued*)

Cell design	Source	Ion recovered	Operation voltage (V)	Energy consumption	System performance	Ref.
Carbon plate electrodes, commercial CEM and AEM	Synthetic wastewater	NO_3^-	0.8	N/A	83.07 % removal efficiency	[142]
Porous carbon electrodes	Groundwater samples, synthetic solutions	NO_3^-	1.5	0.4 kWh/m^3	98 % reduction in concentration, from 233 mg/L to 4.6 mg/L	[143]
AC-based electrode carbon powder, containing Polytetrafluoroethylene emulsion, MCDI + IE process	Synthetic wastewater	NH_4^+	1.2	N/A	Selective ion removal by MCDI increased from 15 % to over 45 % after 5 MCD cycles, The MCDI + IE process recovers >65 % of ammonium after 3 MCDI cycles.	[140]
Ac-based electrode coated with a polymer selective for anions, and polystyrene macroporous A520E resin particles	Synthetic water synthetic sample, municipal wastewater	NO_3^-	1.2	N/A	A greater NO_3^- selectivity resulted in the removal of 81.5 % of NO_3^- from actual municipal wastewater.	[127]
AC electrodes coated by cation- and anions selective ion-exchange polymers	Municipal wastewater	NO_3^-	1.2	N/A	91.08 % removal efficiency in the pilot scale	[128]

– Optimal values were selected for operation voltage and energy consumption voltage when reported; otherwise, data represents standard conditions.

enhancing the removal of NO_3^- and overall system efficiency. In a study presented by Jiang et al. [129], the investigation focused on the performance of AC electrodes in CDI. The study analyzed the effects of flow rate, applied voltage, and the concentration of the initial solution on ion removal. The AC electrodes were chemically modified by phosphoric acid (ACP), resulting in increased specific surface area by 10.71 %, mesopore ratio by 14.69 %, and micropore ratio by 24.06 %. The electrosorption load reached a high value of 19.28 mg/L. Both AC and ACP electrodes showed a decrease in nitrate removal efficiency as the initial feed solution concentration increased. As the initial feed solution concentration increased, nitrate removal efficiency decreased while the unit electrosorption load gradually improved for both AC and ACP electrodes.

Gao et al. [130] developed an innovative CDI system called inverted capacitive deionization (i-CDI), where an anode has net negative surface charges and a cathode has net positive surface charges. The system differs from conventional CDI systems in that it separates salt in an opposing manner. When charged with power, the cathode and anode separate the cations and anions. The i-CDI focuses on enhancing the net surface charges of carbon materials to improve the salt separation performance of the i-CDI system. In the i-CDI, ions are adsorbed onto electrodes solely due to the chemical charges present on the electrode surfaces, without the need for an external voltage. Accordingly, Palko et al. [131] introduced a novel CDI cell design using surface charge for nitrate removal. Their functionalized electrodes, treated with a surfactant containing a quaternary amine ionic group, demonstrated effective removal of ionic pollutants. This hybrid CDI system enables automated electrical regeneration and reduces waste disposal. The functionalized surfaces can be regenerated multiple times by applying an electrostatic potential, removing bound nitrate ions while maintaining excess electronic charge on the electrode. The proposed system combines elements of CDI, with one electrode exhibiting strong capacitive behaviour, while the counter electrode primarily undergoes Faradaic reactions. In their subsequent works [132,133], explored the combination of ion exchange resins with i-CDI operation as a promising method for selective ion removal. They treated the active electrode (cathode) with cetrimonium bromide (CTAB) and the capacitive counter electrode (anode) with sodium dodecyl benzene sulphonate (SDBS). The CTAB-generated surface charge allowed nitrate adsorption without applying potential, achieving a capacity of approximately 80 mg/g of activated carbon. Regeneration was achieved by applying a 3 V potential, causing electrons to migrate from the SDBS-treated electrode to the CTAB-treated electrode, repelling Na^+ and ions. The i-CDI system effectively removed nitrate, with a maximum of over 10 mg of sodium nitrate removed per gram of both electrodes. Additionally, it showcased the potential to substitute the Faradaic titanium counter electrode from previous work with an SDBS-treated capacitive counter electrode, leading to a fully integrated i-CDI cell. This modification substantially improved the energy efficiency of nitrate removal by 1 to 2 orders of magnitude. Oyarzuna and colleagues [133] introduced a nitrate-selective i-CDI system that utilized a straightforward electrode functionalization method with ionic exchange resins, specifically quaternary amine surfactants. Different from the limited system outlined by Palko et al. [131] which depended solely on a single functionalized electrode, they enhanced their approach by functionalizing both electrodes. This advancement led to the creation of a more comprehensive i-CDI cell. This innovative system demonstrated enhanced nitrate selectivity at lower voltages, effectively reducing $NaNO_3$ concentrations from approximately 170 ppm to levels below the permissible limit for nitrate in drinking water. The researchers further investigated the selectivity of nitrate compared to chloride ions based on the regeneration voltage and initial chloride concentration. An operational method for CDI/i-CDI was introduced, which focuses on increasing water recovery while also enhancing the concentration of high-affinity species, such as nitrate, in comparison to lower-affinity species like chloride. Additionally, they developed a model to explain the behaviour of functionalized electrodes in terms of the adsorption and regeneration capabilities within the i-CDI system.

By using electrodes made from nanosheet-like graphene laminates (GL) in an MCDI, Wimalasiri et al. [26] compared the effectiveness of removing and adsorbing sodium (Na^+) and ammonium (NH_4^+) ions. As a result, the GL-based electrodes were able to remove 15.3 mg/g of NH_4Cl, while NaCl could be removed at 14.3 mg/g. Using the pseudo-first-order kinetic model, they observed NH_4^+ ions adsorbing at a faster rate on GLs than Na^+ ions to understand the adsorption behaviour of ammonium ions. In addition, NH_4Cl electrosorption did not appear to be significantly affected by Na^+ ions in a mixture of Na^+, suggesting NH_4Cl has a faster adsorption rate than NaCl. Hawks and colleagues [134] conducted a study to examine the correlation between highly selective nitrate adsorption and pore size distribution using an ultramicroporous aerogel monolith (μHCAM) as an electrode in CDI. Through molecular dynamics simulations, they observed that nitrate exhibited a strong preference for electro-sorption over sulphate and chloride due to the presence of tightly distributed micropores, predominantly <1 nm. These narrow pores were found to facilitate the adsorption of the planar, weakly hydrated nitrate molecule and resulted in increased capacitance for nitrate compared to chloride. Furthermore, in the presence of sulphate as the sole anion, significant ion-sieving effects were observed, further highlighting the advantages of the narrow pore structure in μHCAM [134].

The inclusion of metal oxides in hybrid electrodes is crucial for enhancing efficiency by optimizing the surface area for salt electrosorption. This optimization considers various pore types and incorporates hydrophilic characteristics to fulfil the total existing pore

Table 3
System design for FCDI-based Systems for selective recovery from wastewater.

Cell architecture	Cell design	Source	Ion recovered	Operation voltage (V)	Energy consumption	System performance	Ref.
FCDI	Ac-based electrode combined with $K_2Ti_2O_5$ (KTO) particles	Synthetic wastewater	NH_4^+	NA	2.490 kWh/kg N	64.8 % removal efficiency, and over 80 % desorption efficiency	[153]
FCDI	Carbon-based electrode, Commercial AEM/CEM	Diluted wastewater	NH_4^+	~0.8	94.4 kWh/kg and 79.5 kWh/kg for different carbon contents	Selectivity range of 3.7 to 11.4 for ammonium ions compared to other cations (Na^+, K^+, and Ca^{2+}).	[152]
FCDI	Commercial AC, CEM, and AEM	Synthetic wastewater	NH_4^+	1.2	N/A	87 % efficiency in removing ammonia, an adsorption capacity of 1.43 mg NH_4Cl/g, and yielded a 322.06 mg N/L final ammonia concentration	[144]
FCDI	Mixing NH_4Cl (or NaCl) solutions with AC, CEM-DF-120, and AEM for flow-electrode suspension.	Synthetic wastewater	NH_4^+	1.2	N/A	Efficient ammonia removal involves maintaining an initial Concentration Factor (CF) below 10	[147]
Stacked FCDI	Mixing commercial AC in deionized water with carbon cation-selective exchange membrane	Synthetic wastewater with NH_4Cl, $MgCl_2$, and $CaCl_2$	NH_4^+	1.2	887 J/mmol	Noteworthy enhancement in the purity of the ammonium sulphate product (rising from around 50 % to 85 %), accompanied by an almost twofold increase in the ratio of NH_4^+ ions to co-existing cations	[151]
FCDI	AC-based electrode, commercial IEM	Highly concentrated digestate wastewater, Synthetic solutions	Ammonia gas	1	N/A	89 % removal efficiency for synthetic digestate wastewater and 67 % for real digestate wastewater.	[149]
FCDI	AC/Mxene-based electrode	Simulated agricultural wastewater.	NH_4^+	1.2	0.45 kWh/kg	60 % removal efficiency, and 460 mg/g an adsorption capacity	[160]
HCDL	Two copper hexacyanoferrate (CuHCF) battery electrodes, commercial AEM	Synthetic wastewater, actual domestic wastewater	NH_4^+	0.1, 0.2	1.5 kWh/kg N	Selectivity (ratio of per cent removed of $NH_4^+/Na^{+)} > 5$ for synthetic wastewater, selectivity >4 for actual domestic wastewater (85 % removal)	[11]
HCDL	CuHCF-based electrodes	Synthetic and actual industrial wastewater l	NH_4^+	0.79 ± 0.03	0.34 Wh/g NH_4^+ from the synthetic stream, and 0.40 Wh/g NH_4^+ for industrial steam	High NH_4^+ removal efficiencies of 95 % and 93 % for the synthetic and industrial streams, respectively.	[163]
HCDI	NiHCF-based electrode	Municipal wastewater	NH_4^+	0.8	0.3 kWh/kg	Preference for intercalation of NH_4^+, followed by K^+, Na^+, Ca^{2+}, and Mg^{2+}	[154]
HCDI	CNT/N-CuHCF	Synthetic solution	NH_4^+	1.2	126.1 kJ/mol NH_4Cl^{-1}	High specific adsorption capacity (120.2 mg/g), and remarkable long-term durability (no significant decay observed over 100 cycles)	[56]
HCDL	Five distinct MHCFs (M is Ni, Cu, Fe, Co, or Zn)	Synthetic solution	NH_4^+, Na^+	−1.0 V/0.5 V for most of the HCDI, and −0.8 V/0.8 V for AC//FeHCF-HCDI	0.016 kWh/mol	Significant selectivity of all MHCF electrodes for NH_4^+ over Na^+ (>4), significant performance of NiHCF electrode	[159]
FCDI-GPM* contactor	CEM and AEM sheets made from acrylic with carved serpentine channels	Dilute synthetic wastewater	NH_4^+	<1.0	At 11.5 A m^{-2} current density (HRT: 1.48 min), ammonia recovery consumed 21.7 kWh/kg of N with 55.1 % efficiency.	90 % removal efficiency, and 60 % recovery efficiency	[13]
FCDI-FGPM**	CEM and AEM sheets made from acrylic with carved serpentine channels	Dilute and concentrated wastewater	NH_4^+	0 < V < 4	2.1 kWh/kg for domestic wastewater and 7.8 kWh/kg for synthetic wastewater	90 % removal efficiency, and 80 % recovery efficiency	[161]
FCDI/Flow cathode (FC)	Cu@AC flow electrode, commercial CEM and AEM, and Cu@AC flow cathode	Synthetic groundwater	NO_3^-, Cl^-, SO_4^{2-}	NA	NA	Efficiently achieving cation removal, nitrate capture and reduction, and ammonia generation without the need for extra chemicals or electrolytes.	[162]

– Optimal values were selected for operation voltage and energy consumption voltage when reported; otherwise, data represents standard conditions.
* Gas-permeable hollow fibre membrane contactor.
** Flat sheet gas permeable membrane.

Table 4
System design for CDI-based systems for selective recovery of phosphorous from wastewater.

Cell architecture	Cell design	Source	Ion recovered	Operation voltage (V)	Energy consumption	Removal/recovery performance	Ref.
CDI	Commercial CDI	Synthetic wastewater	PO_4^{3-}	1.5	1.65 kWh/m^3	Highest removal of phosphate at 86.5 %	[166]
CDI	Anode: ZnZr-COOH/CNT composite, cathode: AC electrode	Synthetic wastewater	PO_4^{3-}	1.2	0.0075 kWh/g P	Excellent adsorption capacity for phosphate at low concentrations across a broad pH of 3–10, resulting in an equilibrium concentration of phosphate at 0.3 mg/L	[169]
CDI	Ac-based electrodes	Synthetic wastewater	PO_4^{3-}	3.6	0.075 kWh/m^3	Maximum adsorption capacity of 8.53 mg/g	[167]
CDI	Ac-based electrodes	Potassium dihydrogen phosphate (KH_2PO_4) solution	PO_4^{3-}	1.8	N/A	Extensive phosphate adsorption capacity achieved by pores within the range of 1.1–3.5 nm	[172]
CDI	MgAl-LDHs/AC electrode.	Potassium dihydrogen phosphate (KH_2PO_4) solution	PO_4^{3-}	1.2 V	N/A	Significantly increased phosphate uptake capability (from 7.1 to 67.92 mg/g).	[170]
MCDI	CA, AEM-CEM	Synthetic wastewater	HPO_4^{2-}	1.2 V in CV mode, 1 A in CC mode	The higher energy efficiency of CC mode compared to CV mode	In competition with Cl^-, the selective removal of divalent phosphate species (HPO_4^{2-} took place under alkaline conditions (pH 8.0 and 9.0)	[165]
MCDI	Composite carbon electrode	Sodium phosphate buffer solution, synthetic wastewater	PO_4^{3-}	<1.3	N/A	The overall efficiency of P removal was observed to be higher at lower initial solution pH values, co-existing anions selectivity: $Cl^- > SO_4^{2-} > P$	[19]
MCDI	Ac electrode, anion-exchange resin-coated electrode (AE-AC)	NaH_2PO_4 and NaH_2PO_4/NaCl solutions	PO_4^{3-}	1.2	0.034 kWh/mol for AE-AC	A 2.24-fold increase in the selectivity coefficient of P over chloride ions (Cl^-) at the AE-AC compared to the AC electrode.	[168]
MCDI	Ac electrode covered by the covalent organic framework	Synthetic wastewater	$H_2PO_4^-$, HPO_4^{2-}	1.8	N/A	The phosphorus selectivity stands out with values of 3.62, 5.98, and 7.01 in NaH_2PO_4/NaCl, NaH_2PO_4/$NaNO_3$, and NaH_2PO_4/Na_2SO_4 solutions, respectively	[178]
FCDI	Ac-based electrode, commercial CEM and AEM	Synthetic wastewater	$H_2PO_4^-$, HPO_4^{2-}	1.2	N/A	Consistent phosphorus removal efficiency of 97 % even after six cycles	[173]
FCDI	Magnetic carbon particles loaded with different Fe_3O_4 contents and carbon black powder, commercial AEM and CEM	Synthetic municipal wastewater	$H_2PO_4^-$, HPO_4^{2-}	2.2 < V < 1.6	21.8 kWh kg^{-1} P	61.9 % recovery of P from wastewater	[175]
FCDI/FBC*	AC-based electrodes, commercial CEM and AEM	Simple feed solution, synthetic wastewater (simulating the anaerobic digestion supernatant)	$H_2PO_4^-$, HPO_4^{2-}	2	2.98 kWh/kg phosphorus	63 % removing and concentrating in the flow-electrode chamber, immobilized approximately 80 % of P as high-purity vivianite crystals, while also eliminating undesired species	[177]
FCDI	AC-based electrodes, commercial CEM and AEM	Synthetic wastewater containing NaH_2PO_4 and Na_2HPO_4	$H_2PO_4^-$, HPO_4^{2-}	1.2	0.59 kWh/kg P at pH 5 and 1.04 kWh/kg P at pH 9, respectively	When pH is decreased from 9 to 5, the phosphorus removal rate increases 84–104 % from 20.8 to 38.3 mg/min in CC mode and 16.8 to 34.3 mg/min in CV mode.	[174]
FCDI	AC-based electrodes, commercial CEM and AEM	Synthetic wastewater (simulating the phosphoric acid industry wastewater)	PO_4^{3-}	1.2	N/A	Selective separation of phosphorous at 90 %, accompanied by the total removal of sulfate and chloride ions	[176]
HCDL	Mg-Al LDHs/AC/AC electrode for anode, Ac-based electrode for cathode	Synthetic solution	PO_4^{3-}	1.2	N/A	High phosphate adsorption capacity 80.43 mg PO_4^{3-}/g	[171]

– Optimal values were selected for operation voltage and energy consumption voltage when reported; otherwise, data represents standard conditions.
* Fluidized bed crystallization.

volume required for the CDI process. This guarantees the necessary pore volume for effective CDI operation. Based on this hypothesis, Fateminia et al. [135] proposed a strategy to enhance the specific capacitance of carbon-based electrodes to remove nitrate using CDI. They developed a ternary composite electrode by incorporating AC, PVDF (polyvinylidene fluoride), polypyrrole, and ZrO_2. This composite electrode leverages the synergistic effects of electrical conductivity, wettability (hydrophilicity), and adsorption capacity to increase nitrate adsorption in the solution. With the modification of AC using nitrogen-containing compounds such as polyaniline, amine and imine groups were introduced into the structure of the carbon electrode, making it a promising candidate for selective nitrate ion separation. In the batch mode CDI cell, the electrosorption capacity was determined to be 6.01 mg/g, with an optimal nitrate removal efficiency of 60.01 % and a water recovery of 72.94 % achieved. Lado et al. [117] investigated the mechanisms of ion removal through Faradaic reactions using metal oxide-coated electrode composites in CDI. According to their report, such electrodes offer several advantages, including high surface site densities, reduced hydrophobicity of carbon substrates, and increased charge efficiency. Composite metal oxide electrodes, which have asymmetric natural surface potentials, contribute to these benefits. Metal oxide surfaces with different charges reduce co-ion desorption during adsorption and minimize

(a)

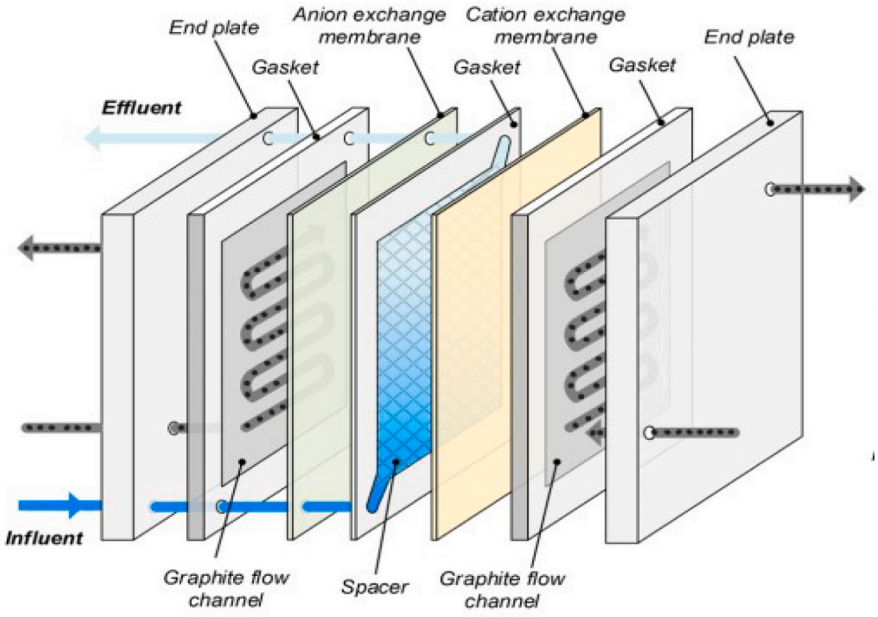

(b)

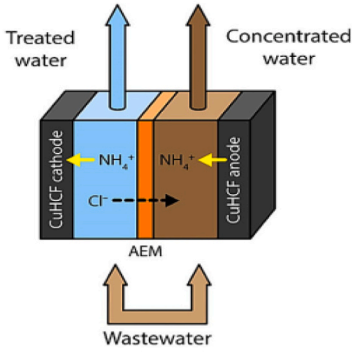

(c)

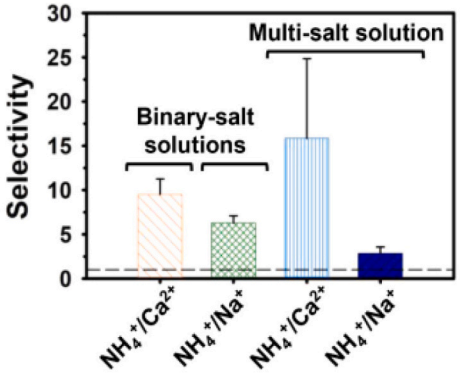

(d)

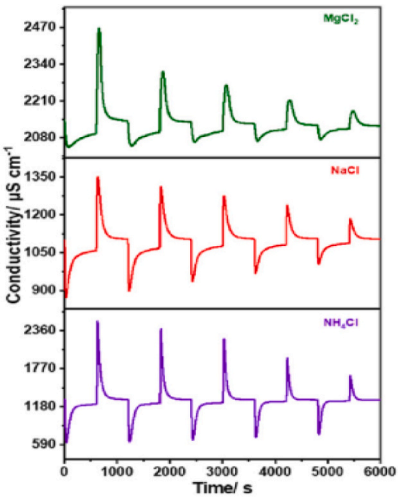

Fig. 4. Schematic representations of (a) A three-chambered FCDI system unit using a flowable electrode and two IEX (AEM and CEM) [152], (b) an HCDI system using two battery electrodes in two channels divided by an AEM [11] (c) Selectivity coefficients of NH_4^+ over competing cations in a NiHCF//activated carbon electrode in binary salt solutions [154], (d) Specific adsorption capacity (SAC) of CNT/N-CuHCF electrode for NH_4^+ ions (performance in NH_4Cl solution is more than twice that in NaCl solution and 5 times that in MgCl2 solution) [56].

counter-ion electrosorption during electrode regeneration, especially in the absence of external potentials. An asymmetric configuration of the CDI cell was used to evaluate low surface area carbons coated with different metal oxides, SiO_2 on the cathode and Al_2O_3 on the anode. In an aqueous environment, these metal oxides were selected based on the contrasting surface charges. SiO_2 particles exhibit a negative charge at a pH above 3, whereas Al_2O_3 particles exhibit a positive charge below a pH of 9. Metal oxide-coated asymmetric carbon electrodes were found to be better at removing nitrate than uncoated symmetric electrodes. It was observed that sodium removal followed a similar pattern to nitrate electrosorption when comparing nitrate coupled with Na^+ or Ca^{2+}, whereas calcium removal was initially slower. As a potential explanation for this observation, they identified a time-dependent ion selectivity within an EDL. Furthermore, the strong affinity of Ca^{2+} ions for SiO_2 particles suggested that calcium adsorbs specifically on the silica-coated electrode in addition to electrosorption within the double layer [117]. Further studies of nitrate electroabsorption in synthetic wastewater have been performed by Gan et al. [136]. They utilized an anion exchange resin (A520E) as the coating layer for the anode and carboxyl-functionalized multi-walled carbon nanotubes (MWCNTs-COOH) as the coating layer for the cathode. Two composite electrodes, A520E/AC and MWCNTs-COOH/AC, were fabricated on general carbon electrodes supported by graphite paper, respectively. The A520E/AC/GP electrode showcased heightened nitrate selectivity, whereas the MWCNTs-COOH/AC/GP electrode demonstrated an increased adsorption capacity. An analysis of anion desorption revealed that nitrate was initially electrostatically adsorbed onto the electrode and subsequently underwent ion exchange within the resin layer. With an increase in applied voltage from 1.0 to 1.6 V, the total amount of adsorbed anions increased, although the molar fraction of nitrate decreased. These findings imply that the adsorption of NO_3^- is influenced by both the electric field and the charged functional group present in the resin.

3.1.1.3. Process development. A new approach has been proposed recently to treat nitrate-concentrated waste liquids that convert nitrate into harmless nitrogen gas, which is an alternative to recovery-based strategies. The NO_3^- adsorbed on the CDI electrode surface and discharged as a concentrated solution in this method converts into N_2 before it is released into the environment. Rogers et al. [137] introduced catalytic CDI (CCDI), utilizing porous carbon as the cathode. Their demonstration revealed that the system achieved a significant 91 % transformation of the adsorbed nitrate into nitrogen gas. They demonstrated that in the CCDI system, nitrate contaminants can be electronically adsorbed and electrochemically reduced, thereby eliminating the concentrated nitrate waste stream in a CDI system. Hu et al. [138] introduced a Pd/NiAl-LMO film electrode for the electrosorption and reduction of NO_3^- in concentrated wastewater. Electro-reduction of the adsorbed NO_3^- to N_2 and intercalation of the original hydrotalcite structure occurred during electrode regeneration.

MCDI shows higher selectivity for removing divalent ions compared to monovalent ions, so it can be effective compared to cation exchange resins for removing ammonium ions [139]. Accordingly, Wang et al. [140] developed a two-stage process using pre-treatment with MCDI followed by ammonium recovery using an ion exchange process. The desalination process of MCDI effectively removed ions and eliminated the negative effects of prior divalent cations like Ca^{2+} and Mg^{2+} on the ion-exchange (IE) absorption-desorption process. The ratio of ammonium to total prior ions in the MCDI outflow significantly increased after several MCDI cycles. Following three cycles of MCDI, a resin regeneration cycle combining MCD and IE recovered over 65 % of ammonium.

3.1.2. FCDI and HCDI

3.1.2.1. Effect of process parameters. In addition to various factors influencing the FCDI process, there is a need for further research and a deeper comprehension of the intricate selectivity associated with the flow electrode. Fang et al. [144] systematically investigated the effect of operational parameters including applied voltage, flow rate, graphite powder dosage, pH value and initial ammonia concentration on the electro-performance of the FCDI for the ammonium recovery. The impact of applied voltage and flow rate was showcased, revealing a significant enhancement in electrosorption performance. The results displayed an increase from 34.45 ± 3.59 % at 0.2 V to 73.48 ± 0.82 % at 1.2 V. Optimization studies on FCDI for desalination processes have emphasized the importance of AC content in system performance [145,146]. Fang et al. [147] discovered that when it comes to ammonia recovery, AC content has a negligible impact on the deionization process. Instead, their research emphasized the importance of optimizing the electrolyte concentration in the FCDI system for effective ammonia recovery. This optimization showed significant impacts on operational expenses, water recovery rate, and energy consumption. The findings were supported by a 720-min long-term experiment conducted on the FCDI cell.

Regarding the significance of applied voltage on the recovery performance of CDI systems and building on the potential of digested liquor as a nitrogen and organic fertilizer [148], Sakar et al. have pioneered an FCDI-based process [149] designed for efficient ammonium recovery from highly concentrated digestate wastewater. Connecting the cell to a vacuum-pressurized vessel containing boric acid facilitated the recovery of ammonia gas generated by the ammonium ions. By increasing the cell voltage and converting ammonium gas to ammonia gas, the researchers could utilize or dispose of the released ammonia gas.

A short-circuited closed cycle (SCC) FCDI was evaluated by Song et al. [150], which focused on nitrate adsorption on activated carbon particles. The findings indicated that FCDI effectively removed nitrate, meeting stringent standards (<1 mg NO_3^-N L^{-1}). However, for cost-effectiveness, a target of 10 mg/L was suggested for high influent nitrate concentrations (50 mg NO_3^-N L^{-1}), requiring less energy (~0.4 kWh/m^3). By replacing the electrolyte periodically and achieving a water recovery rate of 91.4 %, the FCDI system demonstrated continuous desalination performance with effluent nitrate concentrations below typical Maximum Contaminant Levels (MCLs). This was accomplished with minimal energy consumption (approximately 0.5 kWh/m^3) and high productivity (hydraulic retention time, HRT, <1 min). Notably, the study found that using the constant voltage mode was more favourable than conventional CDI systems in maintaining stable effluent quality in SCC FCDI.

3.1.2.2. Cell design. Fang et al. [151] developed a cost-effective stacked FCDI reactor to maximize ammonium ion selectivity over coexisting cations like Ca^{2+} and Mg^{2+}. This design incorporated a monovalent cation-selective exchange membrane (M-CEM) and successfully enabled ammonium sulphate production in the product. Compared to the standard cation exchange membrane (S-CEM), there was a significant improvement in ammonium sulphate product purity, increasing from approximately 50 % to 85 %. Moreover, this improvement led to an almost doubling of the ratio of NH_4^+ ions to co-existing cations.

Using the FCDI configuration (Fig. 4(a)), diluted wastewater was effectively reclaimed into an ammonia solution (NH_3(aq)) through repeated cycles [152]. As an ion exchange membrane is used within the FCDI system, various ions, including ammonium, reach the flowable activated carbon cathode by traversing activated carbon particles. The Faradaic reactions in this cathode caused ammonium to lose protons and become species by favoured ammonium ions. As a result of the FCDI process, ammonia solutions emerged as the primary achievement regarding nitrogen-containing species within the system with selectivity ranging from 3.7 to 11.4 in comparison to other cations [152].

To fabricate a high-efficiency flow electrode, electrospray-activated $K_2Ti_2O_5$ particles (also known as KTO) were combined with AC powder [153]. Through FCDI, a novel KTO-AC flow electrode is designed to

enhance and selectively remove NH_4^+. In typical municipal wastewater, sodium (Na^+) is the predominant coexisting cation, possessing a similar radius of hydration to NH_4^+ (0.358 nm vs. 0.331 nm). As a result, it competes for electrode adsorption. This challenge was addressed by improving the NH_4^+ removal selectivity of mixed KTO-AC flow electrodes. FCDI tests showed an increase in NH_4^+ removal (28.5 % to 64.8 %) and improved desorption efficiency (35.6 % to over 80 %) after incorporating 25 wt% KTO into the electrode mixture. As a result, selective NH_4^+ recovery and efficient electrode regeneration were possible.

The development of an electrode that utilizes Prussian blue analogues (PBAs) to enhance ion selectivity has been the focus of recent research. PBAs possess a crystalline framework with an open structure, enabling the reversible intercalation of ions. The standard formula for PBAs is typically represented as (A_xM_y $[Fe(CN)_6]_z{\cdot}nH_2O$), where M usually signifies a transition metal (such as Mn, Fe, Co, Ni, Cu, and Zn), and A generally denotes the intercalating ions (like Li, Na, K, NH_4, etc.) [155]. To improve the efficiency of the desalination process, nickel hexacyanoferrate (NiHCF) has been developed as an effective PBA [156–158].

Accordingly, Kim et al. [11] presented a BDI process consisting of two copper hexacyanoferrate (CuHCF) capacitive electrodes (that selectively interact with specific ions by Faradaic reactions) that are separated by an anion exchange membrane (Fig. 4(b)). This system selectively removed ammonium ions under low applied voltages ranging from 0.1 to 0.3 V. At an applied voltage of 0.1 V, it achieved a selectivity of >5 (i.e., the ratio of NH_4^+ removed to Na^+ removal), despite the initial higher concentration of Na^+ (20 mM) compared to NH_4^+ (5 mM). The selectivity rose to 9 when employing equimolar concentrations of NH_4^+ and Na^+ (10 mM), suggesting that CuHCF intercalation exhibited a preference for NH_4^+ over other ions. In contrast, using nonselective electrodes (MnO_2) or ion-selective membranes (CuHCF-CEM) showed negligible selectivity (<2). Experiments conducted with actual domestic wastewater demonstrated that the system removed 85 % of NH_4^+ with a selectivity of >4, whereas the removal percentages for other ions were lower (Ca^{2+}: 75 %, K^+: 71 %, Na^+: 20 %, Mg^{2+}: 17 %). The NiHCF electrode exhibited a preference for intercalation NH_4^+, followed by K^+, Na^+, Ca^{2+}, and Mg^{2+}, as observed in municipal wastewater. Among the cations tested, NH_4^+ demonstrated the highest capacity for salt adsorption during consecutive cycles (Fig. 4(c)). These findings suggest that cations characterized by smaller hydrated radii and lower (de)hydration energies were more readily integrated into the NiHCF electrode.

Wang et al. [56] introduced a novel design for a high-performance Faradaic electrode to store NH_4^+ ions in an HCDI system (Fig. 4(d)). The electrode, called CNT/N-CuHCF, exhibited an interconnected nanonetwork structure with a large specific surface area and abundant redox active sites. These features resulted in a high pseudocapacitance contribution and fast ion reaction kinetics. To assess the efficiency of ammonium removal, a batch-mode HCDI module was constructed. AC was used as the anode to capture chloride ions (Cl^-) while PBAs (polybenzoxazole-based adsorbents) served as the cathode to capture ammonium ions (NH_4^+).The CNT/N-CuHCF electrode demonstrated exceptional performance as a CDI electrode for NH_4^+ ion removal, achieving a high specific adsorption capacity (120.2 mg/g), low specific energy consumption (126.1 kJ mol NH_4Cl^-), and remarkable long-term durability (no significant decay observed over 100 cycles). The insights gained from this electrode design contribute to developing high-ammonium removal performance in CDI systems.

HCDI was used to assess the removal, charge efficiency, and selectivity of NH_4^+ and Na^+ ions [159]. The electrochemical characteristics, desalination capacity, stability, and energy use of five distinct MHCF variants were evaluated. Although all MHCF electrodes demonstrated significant selectivity NH_4^+ over Na^+ (>4), the selectivity was unstable because of factors such as electrode structural stability, solution composition, and current density. The NiHCF electrode demonstrated superior performance in terms of specific desalination capacity (~1.23 mmol/g), charge efficiency (>80 %), and stability (82.5 % capacity retention after 50 cycles). Nevertheless, further investigation is necessary to comprehend the ion selectivity behaviour of this electrode type under diverse operational conditions and to assess its recovery performance in the presence of co-existing ions.

Exploiting Mxene's exceptional engineering properties, recent years have witnessed remarkable advancements in its application within aqueous electrochemical energy storage systems. In this context, the incorporation of $Ti_3C_2T_x$ MXene as flow electrodes in an FCDI system has been introduced to improve conductivity and enhance deionization performance [160]. In only 115 min, the $Ti_3C_2T_x$ flow electrodes achieved 60 % ion removal efficiency, demonstrating an adsorption capacity of 460 mg/g. The electrodes were also stable and scalable.

3.1.2.3. Process development. There has been an increased interest in the development of processes to capture nutrient ions and produce value-added products in recent years. Zhang et al. [152] have developed an FCDI system to recover ammonia from dilute wastewater, wherein ammonia successfully migrated through a cation exchange membrane, selectively accumulated in the cathode chamber, and converted into dissolved NH_3. They demonstrated FCDI as a cost-effective method for recovering and utilizing ammonia from wastewater, especially as ammonium sulphate for fertilizers. The captured ammonia was subsequently removed through a membrane contactor and absorbed in an acidic solution such as $(NH_4)_2SO_4$. They combined an FCDI unit with a hydrophobic gas-permeable hollow fibre membrane contactor, achieving 90 % ammonia removal efficiency and 60 % recovery efficiency. They introduced the CapAmm system, which incorporates a flat sheet gas-permeable membrane, to assess ammonia recovery performance from both dilute and concentrated wastewaters. Furthermore, different types of acids (like phosphoric acid or nitric acid) have the potential to be employed in the creation of more valuable fertilizers [161]. The study demonstrated high efficiencies in removing and recovering ammonia, with cost-effective energy consumption, for both low-strength and high-strength wastewaters. The system also achieved stable performance in recovering ammonia and removing salt over a continuous operation period of over two days. Notably, the concentration of ammonia in the system was increased by approximately 80 times compared to the feed stream.

Incorporating a three-chamber FCDI/flow cathode (FC) developed by Sun et al. [162]. Using a single cell facilitates efficient removal of cations, nitrate capture and reduction, and ammonia generation without adding additional chemicals or electrolytes. As the Cu@AC flow electrode acts as both a substrate for nitrate adsorption and as an electrocatalyst for nitrate reduction, the integrated system offers material cost savings. The system illustrates a practical method of treating groundwater with hardness ions.

For preconcentrating low-concentration ammonia in wastewater using FCDI systems, Feng and colleagues [144] achieved an impressive 88 % efficiency in removing ammonia, accompanied by an adsorption capacity of 1.43 mg NH_4Cl/g. This noteworthy performance was observed under 20 mg N/L ammonia concentrations. An ammonia concentration of 322.06 mg N/L was achieved within the flow electrodes using the applied process.

3.2. Phosphorus recovery

Given the stringent phosphorus discharge standards, the imperative is to minimize phosphate introduction into aquatic systems. This poses novel technical hurdles for eliminating phosphorus in wastewater [146]. While a substantial amount of literature exists regarding P recovery from wastewater using carbon-based materials [164], research on the removal using CDI systems, which have demonstrated higher potential, is relatively limited in comparison. The potential of CDI systems will be

explored in the upcoming section.

3.2.1. CDI and MCDI

3.2.1.1. Effect of process parameters. Different P species (PO_4^{3-}, HO_4^{2-}, and $H_2PO_4^-$) dominate depending on the pH of the solution, causing a challenge due to their complexity and variability [165]. Huang et al. [166] conducted a comprehensive study using a commercial CDI system to examine the effects of initial pH, flow rate, and initial concentration on phosphate removal. They determined that the optimal operating condition was a pH value of around 5–6. By utilizing a flow rate of 4.8 L/min, they achieved the highest removal of phosphate at 86.5 % and a significant reduction in conductivity at 81.5 %. The energy consumption for wastewater treatment was calculated to be 7.01 kWh/kg P (removed) or 1.65 kWh/m^3. They subsequently investigated the electrosorption of phosphate using MCDI under two operational modes of constant current (CC) and constant voltage (CV), while varying the initial pH values [165]. The results indicated that the most effective removal of phosphorus occurred at pH 5.0–6.0 when the water solely contained phosphate species. In CC mode, the dominant presence of monovalent phosphate species ($H_2PO_4^-$) resulted in higher energy efficiency compared to CV mode. In CC mode, the study found that in the competitive electrosorption between chloride ions (Cl^-) and phosphate (P), Cl^- was preferentially electrosorbed when monovalent phosphate species (($H_2PO_4^-$) were dominant at pH 5.0 and 6.0. This preference was likely due to Cl^- having a smaller hydrated radius. On the other hand, under alkaline conditions (pH 8.0 and 9.0), the selective removal of divalent phosphate species ($H_2PO_4^-$) took place, primarily driven by their charge characteristic. Therefore, to improve the targeted extraction of P via MCDI from actual wastewater, it might be necessary to employ pre-treatment methods such as pH adjustment and the elimination of co-existing divalent ions.

Jiang et al. [19] conducted a research study to assess the feasibility of effectively removing phosphorus from domestic wastewater, focusing on the pH range of 6.5 to 8.5, which is typically observed in residential raw wastewater. The overall efficiency of P removal was observed to be higher at lower initial solution pH values. According to the study on coexisting anion selectivity, in the presence of higher chloride ion concentrations, phosphate is preferentially removed over chloride due to its greater diffusion strength. Divalent ions like sulphates exhibit a higher electrosorption capacity than similarly concentrated monovalent ions such as phosphate, primarily due to their valence. The preferential electrosorption sequence of the competitive anions present in the wastewater was: $Cl^- > H_2SO_4^{2-} > P$.

It investigated whether process parameters of CDI (voltages, temperatures, and concentrations of P solution) influence electrosorption by examining kinetics, thermodynamics, and equilibrium GCS models [167]. Adsorption rates increased with temperature, voltage, and concentration, with a maximum adsorption capacity of 8.53 mg/g.

Chen et al. [121] evaluated the electrosorption capacity of phosphate (PO_4^{3-}) in mixed electrolyte solutions including Cl^-, NO_3^-, and SO_4^{2-}. They noted a variation in capacity dependent on ionic charge and hydrated radius. The highest capacity was observed for trivalent anions (PO_4^{3-}), followed by divalent anions (SO_4^{2-}), and then monovalent anions (Cl^-, NO_3^-, and F^-). It is worth noting that in typical source water with a neutral pH, phosphate primarily exists as $H_2PO_4^{-2}$, $H_2PO_4^-$, and the dominance of PO_4^{3-} as the primary species occurs only under highly alkaline conditions. Shen et al. [168] investigated the effectiveness of coating carbon with an anion-exchange resin to improve P electrosorption selectivity. As a regenerable method of selective P removal in aqueous solutions, a composite electrode containing an AC electrode and heterogeneous anion-exchange resin is used in an MCDI system. Comparing the coated AC electrode with the uncoated electrode, the thin coating layer s facilitated the preferential transport of phosphate, resulting in a 2.24-fold increase in P selectivity over chloride ions.

Additionally, the electrosorption capacity of P was significantly enhanced and achieved an impressive charge efficiency of 97 % by mitigating the co-ion repulsion effect. Reversible desorption of electro-adsorbed P w has also been demonstrated. Additionally, the study found that P removal was more effective in a single-solute system containing only P as monovalent $H_2PO_4^-$. Divalent HPO_4^{-2} was more competitively removed in a binary-solute system with both P and Cl^-.

3.2.1.2. Cell design. Coexisting ions and pH levels are essential factors in phosphate adsorption. To address this, there is a need to develop a novel material with specific phosphate adsorption properties across a wide pH range. In a CDI system aimed specifically at the removal of phosphate, ZnZr-COOH/CNT, a composite material containing intercalated carbon nanotubes with terephthalic acid was developed as an anode [169]. An analysis was conducted to examine how initial phosphate concentration, pH, applied voltage, and coexisting ions affect adsorption. Excellent adsorption properties were demonstrated by the ZnZr-COOH/CNT electrode, even at phosphate concentrations as low as 10 mg/L and within a pH range of 3 to 10. The equilibrium concentration of phosphate reached as low as 0.3 mg/L. Moreover, the energy consumption of the CDI process for phosphorus removal was remarkably low, calculated at 0.0075 kWh/g P and 0.043 kWh/m^3 of water at an applied voltage of 1.2 V.

Using layered double hydroxide (LDH) electrodes for phosphate removal, Hong et al. [170] introduced a novel electrode that employs multiple mechanisms for phosphate adsorption on the MgAl-LDHs/AC electrode. Physical adsorption occurs via an EDL on the electrode surface, while chemical adsorption occurs through phosphate intercalation and surface complexation. Known as LDHs, they scavenge phosphate through intercalated ion exchange or surface complexation, which makes them ideal for slow-release phosphate fertilizers. The MgAl LDHs/AC electrode exhibited significantly increased phosphate uptake capability (from 7.1 to 67.92 mg/g). Following this, they developed Mg-Al LDHs/AC electrodes to investigate the impact of different experimental parameters on the capacitive removal of phosphate [171]. These electrodes showed a high phosphate adsorption capacity (80.43 mg PO_4^{3-}/g), which increased with higher Mg^{2+}/Al^{3+} ratios. The highest level of phosphate uptake by Mg-Al LDHs/AC was achieved under conditions of near-neutral pH and low ionic strength.

Combining carbon aerogel and AC electrodes with different pore structures was used to analyze the relationship between adsorption capacity and pore size distribution in CDI [172]. The adsorption capacity did not exhibit a direct correlation with traditional pore structure indices. Instead, it was found that the phosphate adsorption capacity strongly correlated with the pore volume and BETSSA in the 1.1–3.5 nm range, highlighting the importance of pores in this size range.

3.2.2. FCDI

3.2.2.1. Effect of process parameters. For optimal FCDI performance for phosphorus removal, a comprehensive investigation of various parameters was conducted [173]. These parameters encompass applied voltage, flow rate, initial phosphorus concentration, and initial pH value. As a result of the results, both the voltage applied and the initial pH value had a profound impact on the removal of phosphorus. When operating under optimal conditions, sustained cycling tests consistently demonstrated a remarkable 97 % phosphorus removal efficiency even after six cycles, showcasing the system's enduring capability in phosphorus removal across cycles. Furthermore, enrichment experiments highlighted the exceptional potential of FCDI in concentrating low-concentration phosphorus solutions from feed water. Within 11 h, the system effectively increased the concentration of the initial 100 mg/L P feed phosphorus solution by a factor of 16. By improving the efficiency of phosphate recovery through the concentration and enrichment of phosphorus-laden wastewater, FCDI has substantiated its competence in

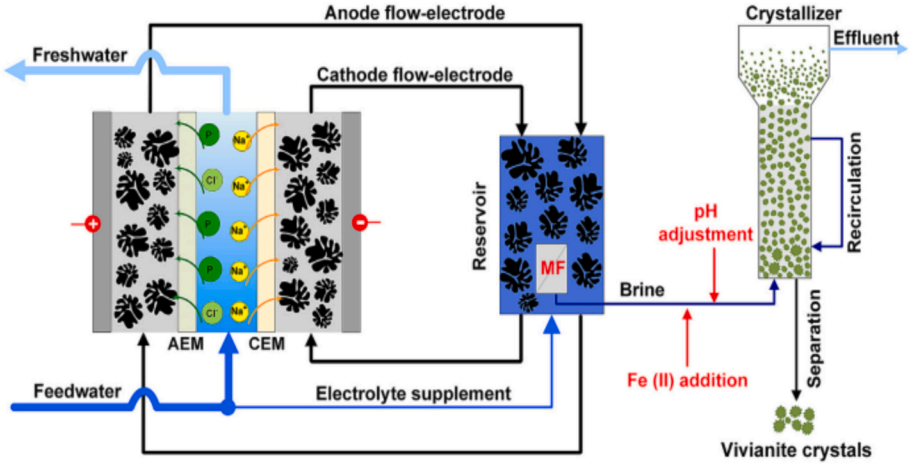

Fig. 5. Schematic representations of FCDI/FBC processes for P recovery as vivianite [177].

phosphate recovery. The behaviour of phosphate ions in the system displayed nuanced responses to pH variations. At a pH range of 2.15 to 7.20, the prevailing phosphate species is primarily $H_2O_4^-$, with the optimal removal efficacy occurring at pH 5. As the pH escalates to 7.20–12.35, HPO_4^{2-} becomes the dominant form of phosphate. Importantly, the diffusion coefficient of $H_2PO_4^-$ surpasses that of HPO_4^{2-}, and the smaller hydration radius of $H_2PO_4^-$ further facilitates its transfer from the spacing channel to the flow electrode. In addition, these results demonstrate that phosphorus removal efficiency through FCDI is largely determined by the initial pH value of the feed water, emphasizing the system's enhanced performance under weakly acidic conditions [173].

Bian et al. [174] investigated phosphate removal using FCDI and examined the impact of pH on the speciation and transport of phosphate ions. They also utilized both CC and CV charging modes in FCDI to

(a)

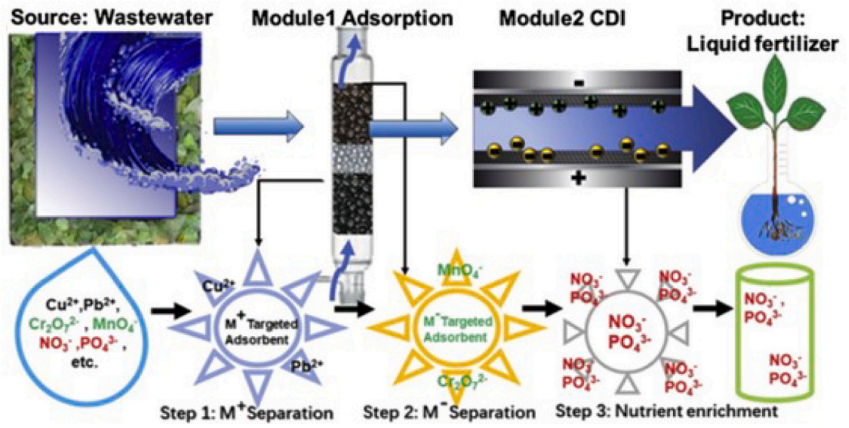

(b)

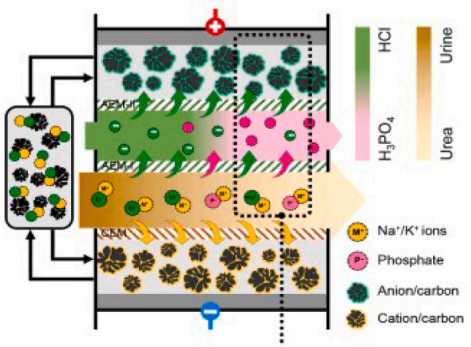

Fig. 6. Schematic illustration of nitrogen (N) and phosphorus (P) recovery from wastewater using (a) a three-stage operation combining adsorption and CDI [25] and (b) an FCDI system utilizing an LMC (liquid membrane chamber) configuration [116].

investigate phosphate removal and energy consumption. They found that lower pH values (pH 5) resulted in higher phosphorus removal rates and reduced energy consumption than higher pH values (pH 9). This improvement was attributed to a shift in dominant phosphate species. In their study, Zhang et al. [163] investigated the influence of current density, hydraulic retention time (HRT), and electrolyte salinity on salt removal and phosphorus recovery in FCDI [175]. They observed a slight increase in cell voltage with higher current densities and found that P and Cl removal efficiency improved with increased HRT. The magnetic carbon particles exhibited a strong affinity for P but no preferential adsorption for Cl^-, indicating their potential for selective phosphorus adsorption.

3.2.2.2. Cell design. To enhance the efficacy of the CDI electrodes, researchers directed their efforts towards the modification of the AC electrodes. They prepared and applied magnetics AC particles impregnated with iron oxide (Fe_3O_4) as FCDI electrodes. These particles were chosen for their relatively high surface area, good electrical conductivity, reasonable static adsorption capacity, and magnetization response. Due to the strong affinity of magnetic carbon electrodes for P, P was selectively adsorbable to the magnetic particles through ligand exchange. This allowed for the effective extraction of 61.9 % of P from wastewater while maintaining a reasonable electrical energy cost of 21.8 kWh/kg P. Furthermore, the study demonstrated that a 4-day continuous experiment could be achieved. An external magnetic field could separate the electrode particles from the brine stream in just three minutes. This process involved utilizing the magnetic properties of the carbon particles. By employing a magnetic field, the researchers were able to easily separate the magnetic particles, resulting in a P-rich stream. The P-loaded magnetic carbon electrode particles could then be regenerated using an alkaline solution [175].

3.2.2.3. Process development. Epshtein et al. [176] proposed an approach to recovery of H_3PO_4 from acidic wastewater containing high levels of Cl^- and SO_4^{2-}, considering pH=2 on the thermodynamic equilibrium of this process [60,174]. Under acidic conditions, the negatively charged Cl^- ions are expelled from the flow-electrode chamber, while the uncharged H_3PO_4 is hindered by an AEM. They introduced a novel two-step process. In the first step, the solution is treated in a stirred batch silica reactor, which aims to remove fluoride ions. In the second step, the SiO_2-treated solution was desalinated using the FCDI technique until complete elimination of chlorine and sulfur species, resulting in 90 % of the phosphorus remaining in the desalinated stream. During this process, uncharged H_3PO_4 becomes dominant in the wastewater's phosphate system.

The research aimed to recover phosphorus as a value-added product through an integrated FCDI/fluidized bed crystallization (FBC) column process. The focus was on converting P into vivianite, which holds promise as a slow-release fertilizer and a reagent for Li-ion secondary batteries (Fig. 5) [177]. Due to the low concentration of P and the presence of other co-existing species, P-rich wastewater was pre-concentrated via FCDI, subsequently leading to immobilization as high-purity vivianite crystals in the FBC column. A flow-electrode chamber efficiently removed and concentrated 63 % of P under optimal conditions. The FBC system successfully immobilized approximately 80 % of P as high-purity vivianite crystals, while also eliminating undesired species, enabling the effective recovery of P in the subsequent FBC system.

3.3. Concurrent recovery of nitrogen and phosphorus

In a CDI study, nitrogen and phosphorus were simultaneously removed and recovered from wastewater [14], but there is a continued need for the development of systems that yield confirmed results in effectively addressing both ions. Ge et al. demonstrated that CDI used as a post-treatment after anaerobic treatment, offers multiple benefits [36]. The research demonstrated notable removal efficiencies, ranging from 77.5 % to 91.2 % for salts, 60.5 % to 95.7 % for ammonium, and 46.4 % to 80.7 % for phosphorus. The application of a low voltage range of 1.2–1.8 V resulted in only a small quantity of phosphate salts being released. This is primarily due to the significant contribution of physical adsorption in removing phosphates, which remains unaffected by the electrical potential difference. A three-stage system combining adsorption and CDI has been developed to recover liquid fertilizers from wastewater (Fig. 6(a)) [25]. Additionally, CDI enabled electro-absorption and desorption processes that enriched nutrients. It was found that plants grown with recovered liquid fertilizers had comparable results to those produced with conventional fertilizers. As well as demonstrating positive effects on plant growth, liquid fertilizers derived from recovered nutrients are also cost-effective [25]. Jiang et al. [179] designed a hybrid system integrating a membrane bioreactor (MBR) and MCDI for recovering nutrients from source-separated urine. The MBR-treated urine served as the feed for MCDI. The study demonstrated removal rates of 66 % for nitrate, 49 % for phosphate, and 58 % for ammonium in the treated urine. Corresponding recovery rates in the concentrated brine were 80 % for nitrate, 64 % for phosphate, and 76 % for ammonium.

In their study, Bian et al. [180] demonstrated the effectiveness of the FCDI process for the simultaneous removal and recovery of salinity, nitrogen, and phosphates from water. They analyzed the distribution of different nitrogen and phosphorus ion species and achieved high removal and recovery rates, including NH_4^+-N (89–99 %), NO_3^--N (83–99 %), and PO_4^{3-}-P (49–91 %). Additionally, implementing a connected flow operation (FCDI-C) led to significant increases in PO_4^{3-}-P removal (43.5 ± 2.2 %), NH_4^+-N removal (12.3 ± 1.1 %), and NO_3^--N removal (9.9 ± 0.3 %). Using a system design strategy for recovering phosphorus and urea, a novel FCDI device was developed, incorporating a liquid membrane chamber (LMC) between the spacer chamber and the anode chamber (Fig. 6(b)) [116]. The LMC was created by employing a pair of parallel AAEMs. During the charging process, the negatively charged P ion (HPO_4^{2-} and $H_2PO_4^-$) were captured by acidic extraction solutions before reaching the anode chamber. A phosphoric acid solution of high purity was then obtained by converting P ions into uncharged H_3PO_4.Undesirable ions such as Cl^- and SO_4^{2-} were simultaneously expelled.

It has been demonstrated by Epshtein et al. [176] that such a mechanism is involved. The FCDI system was also evaluated by examining various operating parameters to determine its performance. These parameters included the ratio of urine volume to extraction solution, urine hydraulic retention time (HRT), current density, and the type of extraction solution. The FCDI system operated continuously for 37.5 h under optimal conditions, achieving satisfactory recovery performance. The obtained phosphorus solution had a concentration of 811 mg/L with a purity of 73.85 %, while the urea-N solution had a concentration of 8.3 g/L with an extraction efficiency of 81.4 %. Son et al. [181] investigated the intercalation capacity of CuHCF electrodes and the extent of phosphate ion removal when chloride ions are present in the BDI process. Compared to the conventional CDI, which typically consumes 4.4–21.7 kWh/kg-N for ammonium recovery, the BDI process stands out for its remarkable efficiency. BDI excels in selectively removing ammonium ions, achieving a removal rate of over 90 % when compared to sodium ions. Furthermore, BDI demonstrates a significantly reduced energy consumption for each unit of nitrogen removed, requiring just 1.5 kWh/kg-N at an applied voltage of 0.2 V, making it a more efficient choice compared to other CDI approaches (Table 5). The study found that CuHCF electrodes consistently and effectively removed ammonium ions, maintaining a stable performance at 8.4 ± 1.4 g-NH_4^+/g-electrode. However, removing phosphate ions proved challenging due to the preferential removal of chloride ions, which were more abundant than phosphate ions.

Gao et al. [182] introduced an innovative approach that combines

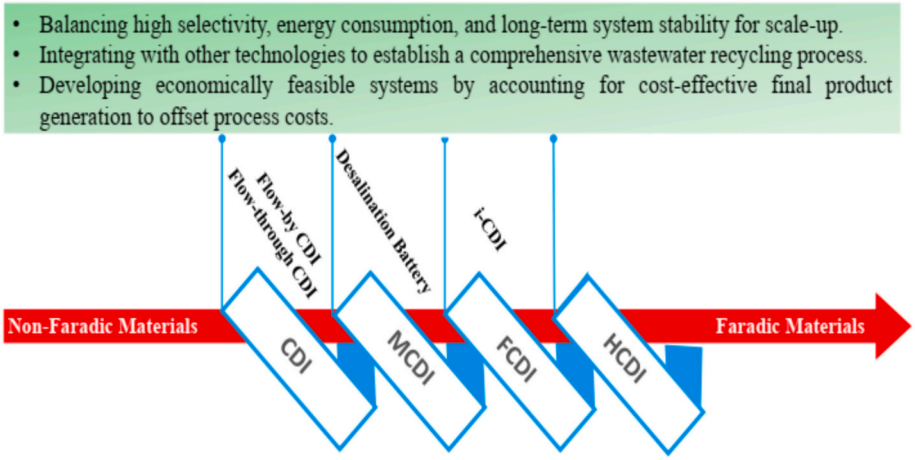

Fig. 7. Graphical summary of the CDI systems progress and key challenges for N, P, and N-P recovery towards the circular economy.

bipolar membrane electrodialysis (BMED) and MCDI to concurrently remove nitrogen and phosphorus from wastewater. BMED facilitates struvite precipitation by regulating the pH of wastewater, while MCDI further decreases ammonia concentrations in the effluent and concentrates excess ammonia. The use of BMED for pH adjustment not only enhances NH_4^+ removal but also diminishes the presence of counter ions in the feed water, minimizing competitive cation consequently alongside NH_4^+. Consequently, this substitution leads to a reduction in energy consumption during NH_4^+ recovery. The results of this approach showcased the removal of approximately 89 % phosphorus and about 77 % ammonia, with roughly 81 % of the wastewater recovered as a high-quality effluent suitable for discharge or reuse.

4. Future perspectives

The CDI system for nutrient recovery has several advantages, including ion selectivity, reduced secondary waste generation, the ability to combine technologies for unique separations, and the production of high-value products. While significant progress has been made in high-performance systems, further advances are needed in system design, process engineering, and recovery mechanisms for these systems to compete with alternatives and overcome techno-economic challenges. Fig. 7 provides a visual summary of the progress and key challenges in the CDI system development for future research, aiming to establish it as a viable commercial solution within the framework of a circular economy.

4.1. Optimization, mechanism, and modeling

Further research is needed to understand the effects of various parameters on CDIs for nutrient recovery, despite extensive literature on process optimization of CDIs (as outlined in the previous sections). Insights into enhancing separation performance can be gained by examining these parameters and their combinations. By doing so, ion selectivity, ion removal rate, electrode adsorption capacity, and energy consumption can be optimized. Nevertheless, while the impact of certain operational parameters, such as the applied voltage on energy consumption or the type of material in electrode performance on adsorption capacity, has been addressed in the current literature, it appears that each operating parameter exhibits distinct effects on CDI cell performance, as reported by various research groups [183–185]. Additionally, the synergistic effect of these parameters should be considered to determine the optimal performance. Consequently, given the limited recent publications in this area [128,161,186], the development of machine learning models to gain a deeper understanding of parameters and the nutrient recovery process is deemed crucial. To ensure long-term stability in the electrode-electrolyte separation process, membrane fouling, and other related issues, fitting modeling techniques should be developed. Furthermore, despite the widespread application of the capacitive mechanism on carbon electrodes and the intercalation mechanism on Faradaic electrodes for selectively separating monovalent ions, there is a notably inadequate understanding and discourse regarding the mechanism of selectivity and durability enhancement in these systems.

4.2. Novel cell design

The potential for significant advancements in efficient nutrient recovery is evident by pioneering innovative electrodes that employ intercalating, chelating, and redox-active materials [12]. In the forthcoming path, integrating diverse chemical groups in a multifunctional manner emerges as a promising strategy to elevate selectivity, surpass current limitations, and establish these materials as a versatile platform for the concurrent extraction of multiple desired elements. Considering the evolution of functionalized electrode materials, attention should also be directed towards enhancing phosphorus (P) recovery [14]. The removal of phosphate has been accomplished using various adsorbents utilizing distinct mechanisms, including lanthanum-based materials [187], iron and iron oxides [188,189], and magnesium hydroxide [190]. These materials have shown promising outcomes and hold potential for incorporation into electrode designs for efficient phosphate removal applications.

Fouling is a concern in CDI devices, manifesting as fouling on electrode surfaces or blockages within electrode pores. In MCDI systems, fouling can also affect membrane surfaces or penetrate the membrane structure [191]. However, an understanding gap exists concerning membrane-related factors influencing CDI systems, encompassing attributes like chemical and physical structure. Challenges of membrane fouling and instability under specific operating conditions, coupled with the diverse parameters in membrane fabrication and processes, necessitate deeper exploration. Promisingly, the development of membranes using techniques like structured nanomaterials [192–194] holds potential for enhancing membrane performance.

Over the past few years, distinct FCDI and HCDI systems have emerged for desalination applications, achieving remarkable results. The design of high-performance FCDI and HCDI cells has been improved through a variety of advanced strategies, and future innovations are expected to be very promising. There is also high potential for nutrient recovery applications in the literature, offering an enticing prospect for future development.

Table 5
System design for CDI-based systems for selective recovery of nitrogen and phosphorous from wastewater.

Cell architecture	Cell design	Source	Ion recovered	Operation voltage	Energy consumption	Removal/recovery performance	Ref.
CDI	Ac-based electrodes	Synthetic solution	NO_3^-, F−, SO_4^{2-}, PO_4^{3-}	1.2	N/A	Preferential order of capacity of trivalent anions (PO_4^{3-}) > divalent anions (SO_4^{2-}) > monovalent anions (Cl^-, NO_3^-, and F^-)	[121]
CDI[1]	Ac-based electrodes	Synthetic solution	NH_4^+, Cl−, SO_4^{2-}, PO_4^{3-}	1.2–3.0	0.045–0.873 kWh/m^3	Removal efficiencies of 60.5–95.7 % for ammonium, and 46.4–80.7 % for phosphorus	[14]
CDI[2]	Commercial carbon cloth	Synthetic wastewater	NO_3^-, PO_4^{3-}	1.2	6.3 kWh/g for N enrichment and 7.3 kWh/g for P enrichment	Efficiently recovering nutrients, removing heavy metals, and producing cost-effective liquid fertilizers from enriched wastewater.	[25]
MCDI	Two CuHCF electrodes, and a commercial AEM	Synthetic wastewater	NH_4^+, HPO_4^{2-}, $H_2PO_4^{2-}$	0.3	<2.4 kWh/kg-N for NH_4^+	As measured by the capacity for removal, it remained relatively unaffected by concentration, and phosphate removal was not preferred over Cl^- removal.	[181]
MCDI[3]	Three identical stacks, each assembly consisting of an AC-based electrode, a commercial AEM, and a CEM.	Synthetic wastewater	NH_4^+, PO_4^{3-}	1.4	1.87 kWh/kg N (1st stage), 2.80 kW h/kg N (2nd stage), and 2.11 kW h/kg N (3rd stage), respectively	Removal of approximately 89 % of phosphorus and about 77 % of ammonia	[182]
MCDI[4]	Ac-based electrodes covered by commercial CEM and AEM	MBR-treated source-separated urine	NO_3^-, PO_4^{3-}, NH_4^+	1, 1.5, 2	3.03 to 11.25 kWh/kg for NH_4^+-N and 3.87 to 14.75 kWh/kg for NO_3^--N.	MCDI-treated urine showed 66 % nitrate removal (80 % recovery), 49 % phosphate removal (64 % recovery), and 58 % ammonium removal (76 % recovery) in the concentrated brine.	[179]
FCDI	Ac-based electrodes, commercial CEM and AEM	Synthetic wastewater	NH_4^+, NO_3^-, and PO_4^{3-}	1, 2	24.1–31.7 kW h/kg for NH_4^+, 8.7–15 kWh/ kg for, and 16.9–29.2 kWh/kg for PO_4^{3-}	Removal and recovery rates of (89–99 %), (83–99 %), and (49–91 %) were significantly enhanced by implementing a connected flow operation (FCDI-C)	[180]
FCDI	Flow-electrode chambers, a liquid membrane chamber (LMC) using commercial AEMs and CEM	Synthetic human urine	Phosphorus and urea	N/A	N/A	Phosphorus solution concentration was 811 mg/L with 73.85 % purity, while urea-N solution concentration was 8.3 g/L with 81.4 % extraction efficiency.	[116]

[1] As a post-treatment after anaerobic treatment.
[2] As a post-treatment after two-stage adsorption treatment.
[3] As a post-treatment after bipolar membrane electrodialysis (BMED).
[4] As a post-treatment after membrane bioreactor (MBR).

4.3. Towards a circular economy

The techno-economic analysis (TEA) has demonstrated that the operational life cycle water costs per cubic meter can be economically viable for selective nitrogen removal within the reported selectivity ranges [195]. In addition, nitrate selectivity of 10 has been shown to reduce life cycle treatment costs to less than $0.2/$m^3$ when using CDI or MCDI systems for nitrate removal [196]. Nevertheless, to foster a circular economy, CDI systems must undergo comprehensive and precise economic evaluations. The following points highlight the critical aspects to be considered in future research:

- To achieve selective purification of complex mixtures and enhance nutrient recovery amidst competing ions, it is critical to gain a comprehensive understanding of electrosorption mechanisms, key operational parameters (such as pH and applied voltage), and pre-treatment methods.
- The development of advanced materials and the implementation of innovative strategies, such as antifouling coatings, are necessary to achieve a desirable balance between uptake, selectivity, and stability. This will enable the transition to industrial-scale systems [192]. Furthermore, in the pursuit of resource optimization and sustainable management practices, Life Cycle Assessment (LCA) serves as a valuable tool to assess the environmental, social, and economic impacts of products and services over their entire lifecycle [197–199]. A study by Cetinkaya et al. [142] emphasizes the need to use environmentally friendly materials in MCDI treatments for the removal of nitrates, thus providing an important signal for the development of material design in this field.
- The trends indicate that FCDI has expanded the scope of possibilities for CDI, bridging the gap between research and practical application. By integrating FCDI with solar cells and microbial fuel cells, further opportunities emerge, and FCDI is more scalable than fixed-electrode CDI [200].
- CDI at an industrial scale requires generating value-added products, such as fertilizers, and removing multifunctional pollutants, such as heavy metals and carbon dioxide [20]. A successful treatment approach and a viable business model for scaling up the process require consideration of these factors. Moreover, research and development are needed to recover other vital nutrients, such as potassium (K) and sulfur (S) [201].
- The trend indicates a growing interest in integrating CDI systems into wastewater management to offer a pragmatic approach to recycling. For instance, the combination of FCDI with reverse osmosis, as an example, has gained attention as it aims to simultaneously tackle desalination and nutrient recovery through continuous treatment—a prospect that has garnered interest from various industries. The development of hybrid systems with highly efficient treatment processes should be a focal point for future research.
- From an energy standpoint, there is a need for theoretical and laboratory investigations to evaluate the energy recovery and economic implications of CDI systems. These studies will help assess energy efficiency, recovery capabilities, and operational parameters to meet wastewater nutrient demands. Moreover, CDI technologies can be

effectively integrated with renewable energy sources, such as solar panels. This integration allows for energy production without relying on external sources, which aligns with sustainable development objectives.

5. Conclusions

In contrast to previous findings that suggested limited selectivity of CDIs in nutrient removal and recovery, this study delved into the literature, focusing on innovations from three fundamental angles: (1) process optimization, (2) cell design, and (3) process development. The research demonstrates that CDI processes can indeed achieve remarkable nutrient recovery efficiency, underscoring their potential as a sustainable technology to address environmental concerns and safeguard valuable resources. This affirmation highlights effective nutrient recovery using CDI systems. It also opens new avenues for their industrial applications and the promotion of circular economy principles. Building upon the innovation trend outlined in Section 2, Section 3 offers a concise and categorized report on the application of CDI systems in nutrient recovery, presented in Tables 2, 3, and 4. However, it appears that four primary research opportunities for nutrient recovery have not been fully explored: (i) The development of HCDI systems utilizing Faraday electrodes to enhance ion selectivity, (ii) Synthesizing materials with improved nitrogen and phosphorus capture capabilities, (iii) Assessing the feasibility of employing high-performance FCDI systems on a pilot scale, given their considerable potential, and (iv) Designing processes to integrate and create hybrid systems, thereby generating value-added products.

Drawing from the present investigation, the positive results obtained in ammonia/ammonium recovery from wastewater via CDI-based systems, particularly when employing hybrid approaches, provide a novel opportunity. However, for phosphorus recovery, the significance of operating parameters in achieving optimal recovery efficiency is evident. Additionally, innovative designs for CDI-based systems (including cell configuration and process treatment) seem promising, potentially opening new avenues in this field. While the literature remains limited to integrated processes for simultaneous N and P recovery, such approaches hold substantial potential in providing economically viable solutions for industrial applications.

CRediT authorship contribution statement

Mohsen Askari: Methodology, Investigation, Formal analysis, Conceptualization. **Saeid Rajabzadeh:** Methodology, Investigation, Formal analysis, Data curation. **Leonard Tijing:** Writing – review & editing, Supervision, Investigation, Formal analysis, Data curation. **Ho Kyong Shon:** Writing – review & editing, Writing – original draft, Validation, Supervision, Resources, Project administration, Methodology, Investigation, Funding acquisition, Formal analysis, Data curation, Conceptualization.

Declaration of competing interest

The authors declare that they have no known competing financial interests or personal relationships that could have appeared to influence the work reported in this paper.

Data availability

No data was used for the research described in the article.

Acknowledgements

This project is supported by the Australian Research Council (ARC) through the ARC Research Hub for Nutrients in a Circular Economy (NiCE) (IH210100001).

References

[1] United Nations, World Population Prospects 2019, Department of Economic and Social Affairs Population Dynamics, 2019.
[2] D.R. Kanter, et al., A framework for nitrogen futures in the shared socioeconomic pathways, Glob. Environ. Chang. 61 (2020) 102029.
[3] Ö. Geyik, M. Hadjikakou, B.A. Bryan, Climate-friendly and nutrition-sensitive interventions can close the global dietary nutrient gap while reducing GHG emissions, Nat. Food 4 (1) (2023) 61–73.
[4] H. Kahiluoto, K.E. Pickett, W. Steffen, Global nutrient equity for people and the planet, Nat. Food 2 (11) (2021) 857–861.
[5] N.D. Mueller, L. Lassaletta, Nitrogen challenges in global livestock systems, Nat. Food 1 (7) (2020) 400–401.
[6] X. Zhang, et al., Quantification of global and national nitrogen budgets for crop production, Nat. Food 2 (7) (2021) 529–540.
[7] M. Xie, et al., Membrane-based processes for wastewater nutrient recovery: technology, challenges, and future direction, Water Res. 89 (2016) 210–221.
[8] W.J. Brownlie, et al., Phosphorus price spikes: a wake-up call for phosphorus resilience, Front. Sustain. Food Syst. (2023) 7.
[9] W.J. Brownlie, et al., Global actions for a sustainable phosphorus future, Nat. Food 2 (2) (2021) 71–74.
[10] T.-L. Chen, et al., Advanced ammonia nitrogen removal and recovery technology using electrokinetic and stripping process towards a sustainable nitrogen cycle: a review, J. Clean. Prod. 309 (2021) 127369.
[11] T. Kim, C.A. Gorski, B.E. Logan, Ammonium removal from domestic wastewater using selective battery electrodes, Environ. Sci. Technol. Lett. 5 (9) (2018) 578–583.
[12] H. Yoon, et al., Review of concepts and applications of electrochemical ion separation (EIONS) process, Sep. Purif. Technol. 215 (2019) 190–207.
[13] C. Zhang, et al., Capacitive membrane stripping for ammonia recovery (CapAmm) from dilute wastewaters, Environ. Sci. Technol. Lett. 5 (1) (2018) 43–49.
[14] Z. Ge, et al., Capacitive deionization for nutrient recovery from wastewater with disinfection capability, Environ. Sci.: Water Res. Technol. 4 (1) (2018) 33–39.
[15] J. Kang, et al., Direct energy recovery system for membrane capacitive deionization, Desalination 398 (2016) 144–150.
[16] R. Zhao, et al., Energy consumption in membrane capacitive deionization for different water recoveries and flow rates, and comparison with reverse osmosis, Desalination 330 (2013) 35–41.
[17] J.-H. Lee, W.-S. Bae, J.-H. Choi, Electrode reactions and adsorption/desorption performance related to the applied potential in a capacitive deionization process, Desalination 258 (1–3) (2010) 159–163.
[18] S. Bao, et al., Application of capacitive deionization in water treatment and energy recovery: a review, Energies 16 (3) (2023) 1136.
[19] J. Jiang, et al., Phosphorus removal mechanisms from domestic wastewater by membrane capacitive deionization and system optimization for enhanced phosphate removal, Process Saf. Environ. Prot. 126 (2019) 44–52.
[20] M. Liu, et al., Recent advances in capacitive deionization: research progress and application prospects, Sustainability 14 (21) (2022) 14429–14461.
[21] S. Dahiya, A. Singh, B.K. Mishra, Capacitive deionized hybrid systems for wastewater treatment and desalination: a review on synergistic effects, mechanisms and challenges, Chem. Eng. J. 417 (2021) 128129–128148.
[22] S. Chai, et al., Selective ion removal by capacitive deionization (CDI)-based technologies, Processes 10 (6) (2022) 1075.
[23] M. Tauk, et al., Ion-selectivity advancements in capacitive deionization: a comprehensive review, Desalination 572 (2024) 117146.
[24] W. Huang, et al., Desalination by capacitive deionization with carbon-based materials as electrode: a review, Surf. Rev. Lett. 20 (6) (2013).
[25] J. Yuan, et al., Simultaneous in situ nutrient recovery and sustainable wastewater purification based on metal anion- and cation-targeted selective adsorbents, J. Hazard. Mater. 382 (2020) 121039.
[26] Y. Wimalasiri, M. Mossad, L. Zou, Thermodynamics and kinetics of adsorption of ammonium ions by graphene laminate electrodes in capacitive deionization, Desalination 357 (2015) 178–188.
[27] Y. Qu, et al., Energy consumption analysis of constant voltage and constant current operations in capacitive deionization, Desalination 400 (2016) 18–24.
[28] L. Legrand, et al., Role of ion exchange membranes and capacitive electrodes in membrane capacitive deionization (MCDI) for CO_2 capture, J. Colloid Interface Sci. 564 (2020) 478–490.
[29] W. Tang, et al., Various cell architectures of capacitive deionization: recent advances and future trends, Water Res. 150 (2019) 225–251.
[30] B. Han, et al., Structure and functionality design of novel carbon and faradaic electrode materials for high-performance capacitive deionization, Chem. Eng. J. 360 (2019) 364–384.
[31] C. Zhang, et al., Faradaic reactions in capacitive deionization (CDI) — problems and possibilities: a review, Water Res. 128 (2018) 314–330.
[32] Y. Oren, Capacitive deionization (CDI) for desalination and water treatment — past, present and future (a review), Desalination 228 (1) (2008) 10–29.
[33] B. Jia, W. Zhang, Preparation and application of electrodes in capacitive deionization (CDI): a state-of-art review, Nanoscale Res. Lett. 11 (1) (2016) 64.
[34] M. Inagaki, Z.-H. Huang, Carbon materials for water desalination by capacitive deionization, New Carb. Mater. 38 (3) (2023) 405–431.
[35] B. Xie, et al., Exploring a sustainable binder for capacitive deionization technology to achieve high salt and zinc ion removal efficiency, Desalination 576 (2024) 117351.
[36] P.M. Biesheuvel, A. van der Wal, Membrane capacitive deionization, J. Membr. Sci. 346 (2) (2010) 256–262.

[37] R. Zhao, et al., Charge efficiency: a functional tool to probe the double-layer structure inside of porous electrodes and application in the modeling of capacitive deionization, J. Phys. Chem. Lett. 1 (1) (2010) 205–210.
[38] S. Porada, et al., Review on the science and technology of water desalination by capacitive deionization, Prog. Mater. Sci. 58 (8) (2013) 1388–1442.
[39] J.-B. Lee, et al., Desalination of a thermal power plant wastewater by membrane capacitive deionization, Desalination 196 (1) (2006) 125–134.
[40] L. Hackl, et al., Electrically regenerated ion-exchange technology: leveraging faradaic reactions and assessing the effect of co-ion sorption, J. Colloid Interface Sci. 623 (2022) 985–991.
[41] S. Al-Amshawee, et al., Electrodialysis desalination for water and wastewater: a review, Chem. Eng. J. 380 (2020) 122231.
[42] Y. Song, et al., Review on current research of materials, fabrication and application for bipolar plate in proton exchange membrane fuel cell, Int. J. Hydrog. Energy 45 (54) (2020) 29832–29847.
[43] W. You, K.J.T. Noonan, G.W. Coates, Alkaline-stable anion exchange membranes: a review of synthetic approaches, Prog. Polym. Sci. 100 (2020) 101177.
[44] R. McNair, G. Szekely, R.A.W. Dryfe, Ion-exchange materials for membrane capacitive deionization, ACS ES&T Water 1 (2) (2021) 217–239.
[45] B.E. Davies, R.I. Davies, A simple centrifugation method for obtaining small samples of soil solution, Nature 198 (4876) (1963) 216–217.
[46] S.-I. Jeon, et al., Desalination via a new membrane capacitive deionization process utilizing flow-electrodes, Energy Environ. Sci. 6 (5) (2013) 1471–1475.
[47] C. Zhang, et al., Integrated flow-electrode capacitive deionization and microfiltration system for continuous and energy-efficient brackish water desalination, Environ. Sci. Technol. 53 (22) (2019) 13364–13373.
[48] J. Lee, et al., Hybrid capacitive deionization to enhance the desalination performance of capacitive techniques, Energy Environ. Sci. 7 (11) (2014) 3683–3689.
[49] H.-R. Park, et al., Surface-modified spherical activated carbon for high carbon loading and its desalting performance in flow-electrode capacitive deionization, RSC Adv. 6 (74) (2016) 69720–69727.
[50] S. Wang, et al., Membrane-free hybrid capacitive deionization system based on redox reaction for high-efficiency NaCl removal, Environ. Sci. Technol. 53 (11) (2019) 6292–6301.
[51] Y. Li, et al., Novel membrane-free hybrid capacitive deionization with a radical polymer anode for stable desalination, Desalination 481 (2020) 114379.
[52] M. Gao, et al., Recent advanced freestanding pseudocapacitive electrodes for efficient capacitive deionization, Sep. Purif. Technol. 324 (2023) 124577.
[53] W. Kong, et al., Highly dispersed ultrasmall BiOCl nanoclusters on graphene sheets as high-performance anion-capture electrode for hybrid capacitive deionization, Desalination 573 (2024) 117222.
[54] F. Beguin, et al., Carbons and electrolytes for advanced supercapacitors, Adv. Mater. 26 (14) (2014) 2219–2251, 2283.
[55] L. Legrand, et al., Solvent-free CO_2 capture using membrane capacitive deionization, Environ. Sci. Technol. 52 (16) (2018) 9478–9485.
[56] S. Wang, et al., CNT/copper hexacyanoferrate: a superior faradic electrode for ammonium ion removal with stable performance and high capacity, Chem. Eng. J. 466 (2023) 143163.
[57] M. Tauk, et al., Recent advances in capacitive deionization: a comprehensive review on electrode materials, J. Environ. Chem. Eng. 11 (6) (2023) 111368.
[58] T. Tawonezvi, et al., Recovery and recycling of valuable metals from spent lithium-ion batteries: a comprehensive review and analysis, Energies 16 (3) (2023) 1365.
[59] D. Miranda, Overview on theoretical simulations of lithium-ion batteries and their application to battery separators, Adv. Energy Mater. 13 (13) (2023).
[60] Z.-H. Huang, et al., Carbon electrodes for capacitive deionization, J. Mater. Chem. A 5 (2) (2017) 470–496.
[61] L. Zou, G. Morris, D. Qi, Using activated carbon electrode in electrosorptive deionisation of brackish water, Desalination 225 (1) (2008) 329–340.
[62] O. Sufiani, et al., Modification strategies to enhance electrosorption performance of activated carbon electrodes for capacitive deionization applications, J. Electroanal. Chem. 848 (2019) 113328.
[63] X. Liu, et al., Nitrogen-doped hierarchical porous carbon aerogel for high-performance capacitive deionization, Sep. Purif. Technol. 224 (2019) 44–50.
[64] P. Xu, et al., Treatment of brackish produced water using carbon aerogel-based capacitive deionization technology, Water Res. 42 (10) (2008) 2605–2617.
[65] G. Wang, et al., Highly mesoporous activated carbon electrode for capacitive deionization, Sep. Purif. Technol. 103 (2013) 216–221.
[66] C. Tsouris, et al., Mesoporous carbon for capacitive deionization of saline water, Environ. Sci. Technol. 45 (23) (2011) 10243–10249.
[67] Y. Bouhadana, et al., Capacitive deionization of NaCl solutions at non-steady-state conditions: inversion functionality of the carbon electrodes, J. Phys. Chem. C 115 (33) (2011) 16567–16573.
[68] L. Guo, et al., The efficient faradaic $Li_4Ti_5O_{12}$@C electrode exceeds the membrane capacitive desalination performance, J. Mater. Chem. A 7 (15) (2019) 8912–8921.
[69] J. Yang, L. Zou, N.R. Choudhury, Ion-selective carbon nanotube electrodes in capacitive deionisation, Electrochim. Acta 91 (2013) 11–19.
[70] A. Aldalbahi, et al., Single-walled carbon nanotube (SWCNT) loaded porous reticulated vitreous carbon (RVC) electrodes used in a capacitive deionization (CDI) cell for effective desalination, Nanomaterials 8 (7) (2018) 527.
[71] H. Li, et al., A comparative study on electrosorptive behavior of carbon nanotubes and graphene for capacitive deionization, J. Electroanal. Chem. 653 (1) (2011) 40–44.
[72] Z. Li, et al., 3D porous graphene with ultrahigh surface area for microscale capacitive deionization, Nano Energy 11 (2015) 711–718.
[73] A. Aghigh, et al., Recent advances in utilization of graphene for filtration and desalination of water: a review, Desalination 365 (2015) 389–397.
[74] J. Kim, et al., Removal of calcium ions from water by selective electrosorption using target-ion specific nanocomposite electrode, Water Res. 160 (2019) 445–453.
[75] P. Nie, et al., Self-supporting porous carbon nanofibers with opposite surface charges for high-performance inverted capacitive deionization, Desalination 520 (2021) 115340.
[76] Q. Dong, et al., Electrospun composites made of reduced graphene oxide and activated carbon nanofibers for capacitive deionization, Electrochim. Acta 137 (2014) 388–394.
[77] C. Nie, et al., Electrophoretic deposition of carbon nanotubes–polyacrylic acid composite film electrode for capacitive deionization, Electrochim. Acta 66 (2012) 106–109.
[78] V. Sharma, et al., Carbon-based electrode materials with ion exchange membranes for enhanced membrane capacitive deionization, Colloids Surf. A Physicochem. Eng. Asp. 676 (2023) 132064.
[79] J. Oladunni, et al., A comprehensive review on recently developed carbon based nanocomposites for capacitive deionization: from theory to practice, Sep. Purif. Technol. 207 (2018) 291–320.
[80] M.M. Taha, et al., Exceptional long-term stability of titanium oxynitride nanoparticles as non-carbon-based electrodes for aerated saline water capacitive deionization, Desalination 546 (2023) 116219.
[81] H.H. Kyaw, et al., Fabrication and utilization of ternary cubical nanostructure modified activated carbon cloth electrodes for capacitive deionization system, Sep. Purif. Technol. 330 (2024) 125436.
[82] T. Wu, et al., Surface-treated carbon electrodes with modified potential of zero charge for capacitive deionization, Water Res. 93 (2016) 30–37.
[83] J. Ma, R. Zhou, F. Yu, Hotspots and future trends of capacitive deionization technology: a bibliometric review, Desalination 571 (2024) 117107.
[84] J.C. Farmer, et al., Capacitive deionization of NH_4ClO_4 solutions with carbon aerogel electrodes, J. Appl. Electrochem. 26 (10) (1996).
[85] B. Zhang, A. Boretti, S. Castelletto, Mxene pseudocapacitive electrode material for capacitive deionization, Chem. Eng. J. 435 (2022) 134959.
[86] F. Dixit, et al., Application of MXenes for water treatment and energy-efficient desalination: a review, J. Hazard. Mater. 423 (2022) 127050.
[87] C. Huyskens, J. Helsen, A.B. de Haan, Capacitive deionization for water treatment: screening of key performance parameters and comparison of performance for different ions, Desalination 328 (2013) 8–16.
[88] S. Porada, et al., Effect of electrode thickness variation on operation of capacitive deionization, Electrochim. Acta 75 (2012) 148–156.
[89] X. Liu, et al., Unlocking enhanced capacitive deionization of $NaTi_2(PO_4)_3$/carbon materials by the yolk–shell design, J. Am. Chem. Soc. 145 (16) (2023) 9242–9253.
[90] Z. Chen, et al., Ti_3C_2 MXenes-derived $NaTi_2(PO_4)_3$/MXene nanohybrid for fast and efficient hybrid capacitive deionization performance, Chem. Eng. J. 407 (2021) 127148.
[91] Y. Zhao, et al., Synergistic improvement in capacitive deionization performance using a novel phase-integrated $Na_{0.55}Mn_2O_4$@$Na_{0.7}MnO_2$, ACS Sustain. Chem. Eng. 9 (6) (2021) 2496–2506.
[92] H. Kanoh, et al., Selective electroinsertion of lithium ions into a platinum/.lambda.-manganese dioxide electrode in the aqueous phase, Langmuir 7 (9) (1991) 1841–1842.
[94] S. Kim, et al., Lithium recovery from brine using a λ-MnO_2/activated carbon hybrid supercapacitor system, Chemosphere 125 (2015) 50–56.
[95] C. Zhao, et al., Porous carbon nanosheets functionalized with Fe_3O_4 nanoparticles for capacitive removal of heavy metal ions from water, Environ. Sci. Water Res. Technol. 6 (2) (2020) 331–340.
[96] S. Yang, M. Luo, In-situ embedding ZrO_2 nanoparticles in hierarchically porous carbon matrix as electrode materials for high desalination capacity of hybrid capacitive deionization, Mater. Lett. 248 (2019) 197–200.
[97] X. Ma, et al., Enhanced desalination performance via mixed capacitive-faradaic ion storage using RuO_2-activated carbon composite electrodes, Electrochim. Acta 295 (2019) 769–777.
[98] S.-H. Lee, et al., Electrosorption removal of cesium ions with a copper hexacyanoferrate electrode in a capacitive deionization (CDI) system, Colloids Surf. A Physicochem. Eng. Asp. 647 (2022) 129175.
[99] Z.Y. Leong, H.Y. Yang, A study of MnO_2 with different crystalline forms for pseudocapacitive desalination, ACS Appl. Mater. Interfaces 11 (14) (2019) 13176–13184.
[100] M. Pasta, et al., A desalination battery, Nano Lett. 12 (2) (2012) 839–843.
[101] T. Kim, C.A. Gorski, B.E. Logan, Low energy desalination using battery electrode deionization, Environ. Sci. Technol. Lett. 4 (10) (2017) 444–449.
[102] W. Wei, et al., Electrochemical driven phase segregation enabled dual-ion removal battery deionization electrode, Nano Lett. 21 (11) (2021) 4830–4837.
[103] K. Sun, Electrocapacitive deionization: mechanisms, electrodes, and cell designs, Adv. Funct. Mater. 33 (18) (2023).
[104] M.M. Al-Rajabi, et al., Capacitive deionization for water desalination: cost analysis, recent advances, and process optimization, J. Water Process Eng. 58 (2024) 104816.
[105] Y. Qi, et al., Recent advances in covalent organic frameworks for capacitive deionization: a review, Electrochim. Acta 479 (2024) 143870.

[106] R.L. Zornitta, L.A.M. Ruotolo, L.C.P.M. de Smet, High-performance carbon electrodes modified with polyaniline for stable and selective anion separation, Sep. Purif. Technol. 290 (2022) 120807.
[107] K. Xu, et al., The polymeric conformational effect on capacitive deionization performance of graphene oxide/polypyrrole composite electrode, Desalination 486 (2020) 114407.
[108] Y. Zhang, et al., Polypyrrole nanowire modified graphite (PPy/G) electrode used in capacitive deionization, Synth. Met. 160 (13) (2010) 1392–1396.
[109] L. Lai, et al., Preparation of supercapacitor electrodes through selection of graphene surface functionalities, ACS Nano 6 (7) (2012) 5941–5951.
[110] L. Liu, et al., Three-dimensional electrode design with conductive fibers and ordered macropores for enhanced capacitive deionization performance, Desalination 498 (2021) 114794.
[111] H. Liu, et al., A polyoxometalate-based binder-free capacitive deionization electrode for highly efficient sea water desalination, Chemistry 26 (19) (2020) 4403–4409.
[112] S. Vafakhah, et al., A review on free-standing electrodes for energy-effective desalination: recent advances and perspectives in capacitive deionization, Desalination 493 (2020) 114662.
[113] M. Ding, et al., Free-standing electrodes derived from metal–organic frameworks/nanofibers hybrids for membrane capacitive deionization, Adv. Mater. Technol. 3 (11) (2018) 1800135.
[114] Y. Bai, et al., Graphene oxide-embedded porous carbon nanofiber webs by electrospinning for capacitive deionization, Colloids Surf. A Physicochem. Eng. Asp. 444 (2014) 153–158.
[115] J. Lee, et al., Hybrid capacitive deionization to enhance the desalination performance of capacitive techniques, Energy Environ. Sci. 7 (11) (2014) 3683–3689.
[116] L. Xu, et al., Selective recovery of phosphorus and urea from fresh human urine using a liquid membrane chamber integrated flow-electrode electrochemical system, Water Res. 202 (2021) 117423.
[117] J.J. Lado, et al., Removal of nitrate by asymmetric capacitive deionization, Sep. Purif. Technol. 183 (2017) 145–152.
[118] W.T. Mook, et al., Removal of total ammonia nitrogen (TAN), nitrate and total organic carbon (TOC) from aquaculture wastewater using electrochemical technology: a review, Desalination 285 (2012) 1–13.
[119] R. Broséus, et al., Removal of total dissolved solids, nitrates and ammonium ions from drinking water using charge-barrier capacitive deionisation, Desalination 249 (1) (2009) 217–223.
[120] Y.-J. Kim, J.-H. Kim, J.-H. Choi, Selective removal of nitrate ions by controlling the applied current in membrane capacitive deionization (MCDI), J. Membr. Sci. 429 (2013) 52–57.
[121] Z. Chen, et al., A study of electrosorption selectivity of anions by activated carbon electrodes in capacitive deionization, Desalination 369 (2015) 46–50.
[122] Y. Li, et al., Effects of the hydration ratio on the electrosorption selectivity of ions during capacitive deionization, Desalination 399 (2016) 171–177.
[123] O. Pastushok, et al., Nitrate removal and recovery by capacitive deionization (CDI), Chem. Eng. J. 375 (2019) 121943.
[124] S.-W. Tsai, et al., Exploring the electrosorption selectivity of nitrate over chloride in capacitive deionization (CDI) and membrane capacitive deionization (MCDI), Desalination 497 (2021) 114764.
[125] Y.-J. Kim, J.-H. Choi, Selective removal of nitrate ion using a novel composite carbon electrode in capacitive deionization, Water Res. 46 (18) (2012) 6033–6039.
[126] J.-H. Yeo, J.-H. Choi, Enhancement of nitrate removal from a solution of mixed nitrate, chloride and sulfate ions using a nitrate-selective carbon electrode, Desalination 320 (2013) 10–16.
[127] D.I. Kim, et al., Efficient recovery of nitrate from municipal wastewater via MCDI using anion-exchange polymer coated electrode embedded with nitrate selective resin, Desalination 484 (2020) 114425.
[128] D.I. Kim, et al., Reuse of municipal wastewater via membrane capacitive deionization using ion-selective polymer-coated carbon electrodes in pilot-scale, Chem. Eng. J. 372 (2019) 241–250.
[129] S. Jiang, et al., Removal of nitrate using activated carbon-based electrodes for capacitive deionization, Water Supply 18 (6) (2018) 2028–2034.
[130] X. Gao, et al., Surface charge enhanced carbon electrodes for stable and efficient capacitive deionization using inverted adsorption–desorption behavior, Energy Environ. Sci. 8 (3) (2015) 897–909.
[131] J.W. Palko, et al., Nitrate removal from water using electrostatic regeneration of functionalized adsorbent, Chem. Eng. J. 334 (2018) 1289–1296.
[132] D.I. Oyarzun, et al., Adsorption and capacitive regeneration of nitrate using inverted capacitive deionization with surfactant functionalized carbon electrodes, Sep. Purif. Technol. 194 (2018) 410–415.
[133] D.I. Oyarzun, et al., Ion selectivity in capacitive deionization with functionalized electrode: theory and experimental validation, Water Res. X 1 (2018) 100008.
[134] S.A. Hawks, et al., Using ultramicroporous carbon for the selective removal of nitrate with capacitive deionization, Environ. Sci. Technol. 53 (18) (2019) 10863–10870.
[135] R. Fateminia, S. Rowshanzamir, F. Mehri, Synergistically enhanced nitrate removal by capacitive deionization with activated carbon/PVDF/polyaniline/ZrO_2 composite electrode, Sep. Purif. Technol. 274 (2021) 119108.
[136] L. Gan, et al., Selective removal of nitrate ion using a novel activated carbon composite carbon electrode in capacitive deionization, Sep. Purif. Technol. 212 (2019) 728–736.
[137] T.K. Rogers, et al., Catalytic capacitive deionization for adsorption and reduction of aqueous nitrate, ACS ES&T Water 1 (10) (2021) 2233–2241.
[138] C. Hu, et al., Nitrate electro-sorption/reduction in capacitive deionization using a novel Pd/NiAl-layered metal oxide film electrode, Chem. Eng. J. 335 (2018) 475–482.
[139] A. Farkaš, M. Rožić, Ž. Barbarić-Mikočević, Ammonium exchange in leakage waters of waste dumps using natural zeolite from the Krapina region, Croatia, J. Hazard. Mater. 117 (1) (2005) 25–33.
[140] Z. Wang, et al., Nitrogen recovery from low-strength wastewater by combined membrane capacitive deionization (MCDI) and ion exchange (IE) process, Chem. Eng. J. 316 (2017) 1–6.
[141] W. Tang, et al., Fluoride and nitrate removal from brackish groundwaters by batch-mode capacitive deionization, Water Res. 84 (2015) 342–349.
[142] A.Y. Çetinkaya, Life cycle assessment of environmental effects and nitrate removal for membrane capacitive deionization technology, Environ. Monit. Assess. 192 (8) (2020).
[143] H.I. Uzun, E. Debik, Economical approach to nitrate removal via membrane capacitive deionization, Sep. Purif. Technol. 209 (2019) 776–781.
[144] K. Fang, et al., Recovering ammonia from municipal wastewater by flow-electrode capacitive deionization, Chem. Eng. J. 348 (2018) 301–309.
[145] P. Liang, et al., Optimized desalination performance of high voltage flow-electrode capacitive deionization by adding carbon black in flow-electrode, Desalination 420 (2017) 63–69.
[146] K.Y. Choo, et al., Electrochemical analysis of slurry electrodes for flow-electrode capacitive deionization, J. Electroanal. Chem. 806 (2017) 50–60.
[147] K. Fang, et al., The impact of concentration in electrolyte on ammonia removal in flow-electrode capacitive deionization system, Sep. Purif. Technol. 255 (2021) 117337.
[148] H. Sakar, et al., Ammonium removal and recovery from real digestate wastewater by a modified operational method of membrane capacitive deionization unit, J. Clean. Prod. 215 (2019) 1415–1423.
[149] H. Sakar, et al., Electro-sorption of ammonium by a modified membrane capacitive deionization unit, Sep. Sci. Technol. 52 (16) (2017) 2591–2599.
[150] J. Song, et al., Implication of non-electrostatic contribution to deionization in flow-electrode CDI: case study of nitrate removal from contaminated source waters, Front. Chem. 7 (2019).
[151] K. Fang, et al., Ammonia recovery from concentrated solution by designing novel stacked FCDI cell, Sep. Purif. Technol. 250 (2020) 117066.
[152] C. Zhang, J. Ma, T.D. Waite, Ammonia-rich solution production from wastewaters using chemical-free flow-electrode capacitive deionization, ACS Sustain. Chem. Eng. 7 (7) (2019) 6480–6485.
[153] L. Lin, et al., Selective ammonium removal from synthetic wastewater by flow-electrode capacitive deionization using a novel $K_2Ti_2O_5$-activated carbon mixture electrode, Environ. Sci. Technol. 54 (19) (2020) 12723–12731.
[154] S.-W. Tsai, D.V. Cuong, C.-H. Hou, Selective capture of ammonium ions from municipal wastewater treatment plant effluent with a nickel hexacyanoferrate electrode, Water Res. 221 (2022) 118786.
[155] B. Wang, Prussian Blue analogs for rechargeable batteries, iScience 3 (3) (2018) 110–133.
[156] M.M. Besli, et al., Performance and lifetime of intercalative water deionization cells for mono- and divalent ion removal, Desalination 517 (2021) 115218.
[157] K. Singh, et al., Nickel hexacyanoferrate electrodes for high mono/divalent ion-selectivity in capacitive deionization, Desalination 481 (2020) 114346.
[158] S. Porada, et al., Nickel hexacyanoferrate electrodes for continuous cation intercalation desalination of brackish water, Electrochim. Acta 255 (2017) 369–378.
[159] Q. Wang, et al., Selective removal of ammonium ions with transition metal hexacyanoferrate (MHCF) electrodes, Desalination 558 (2023) 116646.
[160] N.E. Mansoor, et al., Removal and recovery of ammonia from simulated wastewater using $Ti_3C_2T_x$ MXene in flow electrode capacitive deionization, npj Clean Water 5 (1) (2022) 26.
[161] C. Zhang, et al., Continuous ammonia recovery from wastewaters using an integrated capacitive flow electrode membrane stripping system, Environ. Sci. Technol. 52 (24) (2018) 14275–14285.
[162] J. Sun, S. Garg, T.D. Waite, A novel integrated flow-electrode capacitive deionization and flow cathode system for nitrate removal and ammonia generation from simulated groundwater, Environ. Sci. Technol. 57 (39) (2023) 14726–14736.
[163] R. Gao, et al., Separation and recovery of ammonium from industrial wastewater containing methanol using copper hexacyanoferrate (CuHCF) electrodes, Water Res. 188 (2021) 116532.
[164] C. Macías, et al., Improved electro-assisted removal of phosphates and nitrates using mesoporous carbon aerogels with controlled porosity, J. Appl. Electrochem. 44 (8) (2014) 963–976.
[165] X. Huang, et al., Investigation of pH-dependent phosphate removal from wastewaters by membrane capacitive deionization (MCDI), Environ. Sci. Water Res. Technol. 3 (5) (2017) 875–882.
[166] G.-H. Huang, et al., Capacitive deionization (CDI) for removal of phosphate from aqueous solution, Desalin. Water Treat. 52 (4–6) (2014) 759–765.
[167] F.-F. Chen, et al., Characteristic and model of phosphate adsorption by activated carbon electrodes in capacitive deionization, Sep. Purif. Technol. 236 (2020) 116285.
[168] Y.-Y. Shen, et al., Enhanced electrosorption selectivity of phosphate using an anion-exchange resin-coated activated carbon electrode, J. Colloid Interface Sci. 600 (2021) 199–208.
[169] H. Zhang, et al., Development of novel ZnZr-COOH/CNT composite electrode for selectively removing phosphate by capacitive deionization, Chem. Eng. J. 439 (2022) 135527.

[170] X. Hong, et al., Enhanced phosphate removal under an electric field via multiple mechanisms on MgAl-LDHs/AC composite electrode, J. Electroanal. Chem. 836 (2019) 16–23.
[171] E. Zhu, et al., Influence of various experimental parameters on the capacitive removal of phosphate from aqueous solutions using LDHs/AC composite electrodes, Sep. Purif. Technol. 215 (2019) 454–462.
[172] F.-F. Chen, et al., A quantitative prediction model for the phosphate adsorption capacity of carbon materials based on pore size distribution, Electrochim. Acta 331 (2020) 135377.
[173] J. Zhang, et al., Removal and recovery of phosphorus from low-strength wastewaters by flow-electrode capacitive deionization, Sep. Purif. Technol. 237 (2020) 116322.
[174] Y. Bian, X. Chen, Z.J. Ren, pH dependence of phosphorus speciation and transport in flow-electrode capacitive deionization, Environ. Sci. Technol. 54 (14) (2020) 9116–9123.
[175] C. Zhang, et al., Phosphate selective recovery by magnetic iron oxide impregnated carbon flow-electrode capacitive deionization (FCDI), Water Res. 189 (2021) 116653.
[176] A. Epshtein, et al., Treatment of acidic wastewater via fluoride ions removal by SiO_2 particles followed by phosphate ions recovery using flow-electrode capacitive deionization, Chem. Eng. J. 400 (2020) 125892.
[177] C. Zhang, et al., Phosphate recovery as vivianite using a flow-electrode capacitive desalination (FCDI) and fluidized bed crystallization (FBC) coupled system, Water Res. 194 (2021) 116939.
[178] C. Wang, et al., Effective electrosorption and recovery of phosphorus by capacitive deionization with a covalent organic framework-membrane coating electrode, Desalination 570 (2024) 117088.
[179] J. Jiang, et al., Potential nutrient recovery from source-separated urine through hybrid membrane bioreactor and membrane capacitive deionisation, Desalination 566 (2023) 116924.
[180] Y. Bian, et al., Concurrent nitrogen and phosphorus recovery using flow-electrode capacitive deionization, ACS Sustain. Chem. Eng. 7 (8) (2019) 7844–7850.
[181] M. Son, et al., Recovery of ammonium and phosphate using battery deionization in a background electrolyte, Environ. Sci. Water Res. Technol. 6 (6) (2020) 1688–1696.
[182] F. Gao, et al., Nutrient recovery from treated wastewater by a hybrid electrochemical sequence integrating bipolar membrane electrodialysis and membrane capacitive deionization, Environ. Sci. Water Res. Technol. 6 (2) (2020) 383–391.
[183] C.-C. Hu, et al., How to achieve the optimal performance of capacitive deionization and inverted-capacitive deionization, Desalination 442 (2018) 89–98.
[184] M.W. Saleem, W.-S. Kim, Parameter-based performance evaluation and optimization of a capacitive deionization desalination process, Desalination 437 (2018) 133–143.
[185] Y.-U. Shin, et al., Improving the feasibility and applicability of flow-electrode capacitive deionization (FCDI): review of process optimization and energy efficiency, Desalination 502 (2021) 114930.
[186] A. Soo, et al., Machine learning for nutrient recovery in the smart city circular economy — a review, Process. Saf. Environ. Prot. 173 (2023) 529–557.
[187] X. Liu, et al., Lignin-derived porous carbon loaded with $La(OH)_3$ nanorods for highly efficient removal of phosphate, ACS Sustain. Chem. Eng. 7 (1) (2019) 758–768.
[188] T.J. Daou, et al., Phosphate adsorption properties of magnetite-based nanoparticles, Chem. Mater. 19 (18) (2007) 4494–4505.
[189] Z. Ajmal, et al., Phosphate removal from aqueous solution using iron oxides: adsorption, desorption and regeneration characteristics, J. Colloid Interface Sci. 528 (2018) 145–155.
[190] F. Xie, et al., Removal of phosphate from eutrophic lakes through adsorption by in situ formation of magnesium hydroxide from diatomite, Environ. Sci. Technol. 48 (1) (2014) 582–590.
[191] M.E. Suss, et al., Water desalination via capacitive deionization: what is it and what can we expect from it? Energy Environ. Sci. 8 (8) (2015) 2296–2319.
[192] M.A. Alkhadra, et al., Electrochemical methods for water purification, ion separations, and energy conversion, Chem. Rev. 122 (16) (2022) 13547–13635.
[193] A. Alabi, et al., Review of nanomaterials-assisted ion exchange membranes for electromembrane desalination, npj Clean Water 1 (1) (2018) 10.
[194] A. Razmjou, et al., Design principles of ion selective nanostructured membranes for the extraction of lithium ions, Nat. Commun. 10 (1) (2019) 5793.
[195] S. Hand, J.S. Guest, R.D. Cusick, Technoeconomic analysis of brackish water capacitive deionization: navigating tradeoffs between performance, lifetime, and material costs, Environ. Sci. Technol. 53 (22) (2019) 13353–13363.
[196] S. Hand, R.D. Cusick, Emerging investigator series: capacitive deionization for selective removal of nitrate and perchlorate: impacts of ion selectivity and operating constraints on treatment costs, Environ. Sci. Water Res. Technol. 6 (4) (2020) 925–934.
[197] A.Y. Cetinkaya, L. Bilgili, Life cycle comparison of membrane capacitive deionization and reverse osmosis membrane for textile wastewater treatment, Water Air Soil Pollut. 230 (7) (2019).
[198] X. Lai, et al., Critical review of life cycle assessment of lithium-ion batteries for electric vehicles: a lifespan perspective, eTransportation 12 (2022) 100169.
[199] H.-Y. Shiu, et al., Hotspot analysis and improvement schemes for capacitive deionization (CDI) using life cycle assessment, Desalination 468 (2019) 114087.
[200] F. Yu, et al., A comprehensive review on flow-electrode capacitive deionization: design, active material and environmental application, Sep. Purif. Technol. 281 (2022) 119870.
[201] Y. Liu, et al., Recent progress on the recovery of valuable resources from source-separated urine on-site using electrochemical technologies: a review, Chem. Eng. J. 442 (2022) 136200.